NFATc1 negatively determines chondrocyte differentiation in articular cartilage progenitors

Fan Zhang[1,2], Ying Zhao[1,2], Manqi Wang[3], Bin Zhou[4], Bin Zhou[5], Xianpeng Ge[1,2*]

[1]Xuanwu Hospital, Capital Medical University, Beijing 100053, China;

[2]National Clinical Research Center for Geriatric Diseases, Beijing 100053, China;

[3]Central South University, Changsha, Hunan 410083, China;

[4]Department of Genetics, Pediatrics, and Medicine (Cardiology), Albert Einstein College of Medicine of Yeshiva University, New York 10461, United States;

[5]Shanghai Institute of Biochemistry and Cell Biology, Chinese Academy of Sciences, Shanghai 200031, China.

*Correspond to Dr. Xianpeng Ge, Xuanwu Hospital, Capital Medical University, Beijing 100053, China. Email: xianpeng.ge@xwhosp.org or oralxpge@gmail.com

Running title: NFATc1 in articular cartilage development

Abstract

The origin and differentiation mechanism of articular chondrocytes remain poorly understood. Broadly, the difference in developmental mechanisms of articular and growth-plate cartilage is still less elucidated. Here, we identified that the nuclear factor of activated T-cells cytoplasmic 1 (NFATc1) is a crucial regulator of articular, but not growth-plate, chondrocyte differentiation during development. At the early stage of mouse knee development (embryonic day 13.5), NFATc1-expressing cells were mainly located in the flanking region of the joint interzone. With development, NFATc1-expressing cells generated almost all articular chondrocytes, but not chondrocytes in limb growth-plate primordium. NFATc1-expressing cells displayed prominent capacities for colony formation and multipotent differentiation. Transcriptome analyses revealed a set of characteristic genes in NFATc1-enriched articular cartilage progenitors. Strikingly, the expression of NFATc1 was diminished with articular chondrocyte differentiation, and suppressing NFATc1 expression in articular cartilage progenitors was sufficient to induce spontaneous chondrogenesis while overexpressing NFATc1 suppresses chondrogenesis. Mechanistically, NFATc1 negatively regulated the transcriptional activity of the *Col2a1* gene. Thus, our results reveal that NFATc1 characterizes articular, but not growth-plate, cartilage progenitors and negatively determines articular chondrocyte differentiation at least partly through regulating COL2A1 gene transcription.

Keywords

Articular cartilage; Articular chondrocyte; Progenitors; Differentiation; Transcriptional factor; NFAT

The basic mechanism underlying articular cartilage development, particularly the origin and differentiation of articular chondrocytes, remains poorly understood. It is well appreciated that synovial joint tissues, including the articular cartilage, originate from a distinct group of progenitors from those that generate the limb primary cartilaginous anlagen[1, 2]. GDF5 is one of the genes widely used for tracking synovial joint and articular cartilage development[3]. Using reporter mice, multiple groups have displayed that *Gdf5*-expressing cell lineages form almost all articular chondrocytes[1, 4-6]. As GDF5 is expressed in both interzone cells and its flanking cells at the early stage of joint morphogenesis, current results cannot discriminate which site is the origin of articular chondrocytes. Also, GDF5 expression is greatly diminished at the late stage of embryonic development and almost undetectable in articular cartilage in neonatal mice[3]. Thus, GDF5 cannot be used to track articular cartilage progenitors postnatally.

PRG4 is an articular cartilage progenitor marker in the late stage of synovial joint development[2, 7]. This gene encodes lubricin, a major component of synovial fluid and responsible for joint lubricity[8]. PRG4 is detected from the stage of joint cavitation and is predominantly expressed in the surficial layer of developed articular cartilage[9]. Several studies exploited *Prg4-CreER*^{T2} reporter mice to track postnatal articular cartilage development and identified this gene as a marker for postnatal and adult articular cartilage progenitors[6, 10]. Since PRG4 starts to predominantly express and function at the late stage of articular cartilage development, it does not label the primary progenitors of articular cartilage. Several other molecules, such as *Sox9*, *Dkk3, Tgfbr2*, were also utilized to track articular cartilage and synovial joint development[5, 6, 11], but none of these molecules has been shown to specifically and constantly label articular cartilage progenitors and to be able to distinguish the origin of articular chondrocytes.

In addition to the origin of articular chondrocytes, molecular mechanisms regulating articular chondrocyte differentiation remains largely unknown. In particular, the transcriptional regulation of articular chondrocyte differentiation is far from clear. SOX9 is essential in multiple steps of chondrogenesis, but it was originally and mainly studied in growth-plate chondrocytes[12]. Although SOX9 is also expressed in articular cartilage and is essential for maintaining adult articular cartilage homeostasis[13], its detailed functions and mechanisms in articular cartilage development remain to be elucidated. Also, SOX9 starts to express in mesenchymal cells from the very early stage of limb development before the cartilage template formation and it alone is not sufficient to induce chondrogenesis[12, 14]. Therefore, the identification of a core transcriptional regulator of articular chondrocyte differentiation is paramount for understanding the basic mechanism of articular cartilage development and exploring new strategies for treating disorders of articular cartilage.

The nuclear factor of activated T-cells, cytoplasmic 1 (NFATc1) is one of the five members of the NFAT family, which share a similar DNA binding domain of approximately 300 amino acid residues[15, 16]. NFAT signaling plays a broad function in various physiological and pathological processes, including immune cell differentiation and functions, cardiac valve development, and cancer progression and metastasis[15, 17]. In the skeletal system, NFATc1 is critical for osteoclast differentiation and functions[18, 19] and is also involved in osteoblast differentiation by cooperating with the Osterix gene[20]. Intriguingly, NFATc1 expression was found in the superficial layers of articular cartilage as well and decreased in human osteoarthritic cartilage[21]. Following these studies, we recently identified a function of NFATc1 in restricting osteochondroma formation from entheseal progenitors[22], revealing that NFATc1 is a suppressor of chondrogenesis in these cells.

In this study, we unexpectedly found that NFATc1 constantly labels articular cartilage progenitors throughout embryonic development and postnatal growth. The expression of NFATc1 is diminished with articular chondrocyte differentiation, and suppression of NFATc1 in articular cartilage progenitors is sufficient to induce spontaneous chondrocyte differentiation through regulating the transcriptional activity of the COL2A1 gene. These findings provide novel insights into the identity and origin of articular cartilage progenitors and identify a fundamental function of NFATc1 in determining physiological articular chondrocyte differentiation.

Results

Articular cartilage is derived from NFATc1-expressing progenitors

Following our previous discovery that NFATc1 identifies entheseal progenitors at the site of ligaments inserted onto the bone[22], we unexpectedly found that in *Nfatc1-Cre;Rosa26-mTmG*$^{fl/+}$ dual-fluorescence reporter mice, the majority of articular chondrocytes expressed green fluorescence protein (GFP) at 8 weeks of age [Fig. 1(A, B), 90.55 ± 6.38%, n = 5 mice]. As in this genetic reporter mouse line, both *Nfatc1*-expressing cells and their progenies express GFP, this finding suggests that articular chondrocytes were either expressing *Nfatc1* or derived from *Nfatc1*-expressing progenitors. To clarify the expression pattern of NFATc1 during articular cartilage development, we mapped GFP$^+$ cells in *Nfatc1-Cre;Rosa26-mTmG*$^{fl/+}$ mice at the early stage of knee joint morphogenesis (E13.5), postnatal day 0 (P0), and 2 weeks of age [Fig. 1(A)]. At E13.5, GFP$^+$ cells mainly localized to the flanking region of the joint interzone with only sporadic distribution in the interzone site. We further examined the expression of NFATc1 at this stage by crossing the tamoxifen-induced *Nfatc1-CreER*^{T2} mouse line with *Rosa26-mTmG*$^{fl/+}$ mice to generate *Nfatc1-CreER*^{T2};*Rosa26-mTmG*$^{fl/+}$ reporter mice, in which the real-time expression of NFATc1 could be reflected by GFP shortly after tamoxifen pulse. The localization of *Nfatc1*-expressing cells surrounding the joint interzone was verified after administering tamoxifen to *Nfatc1-CreER*^{T2}*;Rosa26-mTmG*$^{fl/+}$ mice at E11.5 and sampling at E13.5 [Supplementary (S) Fig. S1(A)].

In neonatal *Nfatc1-Cre;Rosa26-mTmG*$^{fl/+}$ mice (P0), GFP$^+$ cells consisted of a portion of cells in the presumptive articular cartilage site [Fig. 1(A)]. Strikingly, at 2 weeks of age, most articular chondrocytes turned out to be GFP$^+$, similar to that at 8 weeks of age [Fig. 1(A)]. To clarify the real-time expression of NFATc1 in articular cartilage at 2 weeks and 8 weeks of age, we used

Nfatc1-CreER^{T2};Rosa26-RFP$^{fl/+}$ reporter mice, in which the expression of NFATc1 is reflected by red fluorescence protein (RFP) shortly after tamoxifen administration. Of interest, with tamoxifen pulse, RFP$^+$ cells were found scattered in the articular cartilage at 2 weeks of age accounting for about 22.75 ± 2.18% (*n* = 3 mice) of all cells of articular cartilage, while most RFP$^+$ cells were confined to the superficial layers of articular cartilage at 8 weeks of age (10.94 ± 1.26%, *n* = 3) [Fig. 1(C, D)]. Furthermore, the expression pattern of NFATc1 in mouse articular cartilage was verified by immunohistochemistry at E13.5, P0, 2 weeks, and 8 weeks of age [Fig. 1(E) and Fig. S1(B)]. Therefore, by mapping GFP and RFP expression in articular cartilage of *Nfatc1-Cre;Rosa26-mTmG$^{fl/+}$* and *Nfatc1-CreER^{T2};Rosa26-RFP$^{fl/+}$* mice respectively [Fig. S1(C)], many GFP$^+$ articular chondrocytes in *Nfatc1-Cre;Rosa26-mTmG$^{fl/+}$* mice at 2 weeks and 8 weeks of age should be derived from *Nfatc1*-expressing progenitors and had lost the expression of NFATc1 with development.

Notably, there were no GFP$^+$ chondrocytes in the primordium of growth-plate cartilage at E13.5 in both *Nfatc1-Cre;Rosa26-mTmG$^{fl/+}$* and tamoxifen-induced *Nfatc1-CreER^{T2};Rosa26-mTmG$^{fl/+}$* mice [Fig. 1(A) and Fig. S1(A)], suggesting that NFATc1-expressing cells do not generate the cartilaginous primordium of growth-plate. We did not detect GFP$^+$ cells in articular cartilage in *Rosa26-mTmG$^{fl/+}$* control mice and *Nfatc1-CreER^{T2};Rosa26-mTmG$^{fl/+}$* mice without tamoxifen induction [Fig. S1(D)], suggesting that there was no Cre leakage in the articular cartilage in these two reporter mouse lines. Together, these results reveal that articular chondrocytes are derived from NFATc1-expressing progenitors and NFATc1 expression is diminished with articular cartilage development.

Colony formation and multipotent differentiation of NFATc1-expressing progenitors

The lineage tracing data in *Nfatc1-Cre* and *Nfatc1-CreER^{T2}* reporter mice suggest that NFATc1 characterizes articular cartilage progenitors. In this context, the fluorescence-labeled cells after tamoxifen-induced recombination in *Nfatc1-CreER^{T2}* reporter mice should be able to form *in vivo* cell clones in or next to the articular cartilage with development. To verify this assumption, we exploited the *Nfatc1-CreER^{T2};Rosa26-mTmG$^{fl/+}$* double-fluorescence reporter mouse line and administered two dosages of tamoxifen to dams at P0 and P1 respectively. One week following tamoxifen pulse, GFP^{+} cells were detected at the presumptive articular cartilage site at the mouse knee [Fig. 2(A)]. Local GFP^{+} cell clusters with 3-6 cells each could be observed in articular cartilage by 2 weeks and 8 weeks of age [Fig. 2(A, B)]. Notably, GFP^{+} cell clusters were also found in the meniscus and synovial lining [Fig. 2(A, B)], suggesting that NFATc1 also marks progenitor cells for joint tissues other than articular cartilage. Indeed, in *Nfatc1-Cre;Rosa26-mTmG$^{fl/+}$* mice, GFP^{+} cells also formed the meniscus, synovial lining, and the primordium of the patella at the knee [Fig. 1(A) and Fig. 2(C)].

To further characterize the colony formation capacity of NFATc1-expressing articular cartilage progenitors, we cultured and sorted GFP^{+} cells and their counterparts (GFP^{-} cells) from the knee of neonatal *Nfatc1-Cre;Rosa26-mTmG$^{fl/+}$* mice [Fig. 3(A)]. The *ex vivo* colony formation assay showed that GFP^{+} cells formed remarkably more numerous and larger cell clones in comparison with GFP^{-} cells when plated at the same cell densities and cultured for the same time period [Fig. 3(B)]. A similar outcome could be observed even after five consecutive cell passages [Fig. S2(A)]. Thus, NFATc1-expressing articular cartilage progenitors display a rigorous capacity of colony formation both *in vivo* and *ex vivo*.

To study the differentiation potentials of NFATc1-expressing articular cartilage progenitors, we put GFP^+ and GFP^- cells under chondrogenic, osteogenic, and adipogenic differentiation conditions, respectively. Notably, GFP^+ cells displayed a much higher potential to differentiate towards chondrocytes, osteoblasts, and adipocytes compared to GFP^- cells [Fig. 3(C-E)]. A more striking difference was noticed under the context of chondrocyte differentiation: in the 3D cell-pellet culture model, GFP^+ cells always grew into larger pellets as shown by the diameter of cell pellets and displayed a robust capacity of chondrocyte differentiation as shown by alcian blue staining and COL2A1 protein expression, while GFP^- cells formed relatively small pellets and only displayed faint cartilage formation at the margin of cell pellets [Fig. 3(C)], indicating that GFP^+ cells have a more prominent capacity for proliferation and chondrogenesis compared to GFP^- cells. Furthermore, when transplanted alongside with Matrigel matrix underneath the dorsal skin of SCID mice, these GFP^+ cells differentiated and formed typical chondrocytes as well as chondrocyte clusters within 4 weeks, while the formation of chondrocytes was rarely observed when transplanting GFP^- cells [Fig. 3(F) and Fig. S2(B)]. Notably, many chondrocyte clusters from GFP^+ cells had formed calcified tissues around them, similar to the physiological process of articular cartilage development [Fig. 3(F)].

Taken together, these results demonstrate the intrinsic capacities of colony formation and multipotent differentiation of NFATc1-expressing articular cartilage progenitors.

Transcriptional profile of NFATc1-enriched articular cartilage progenitors

Next, we sought to dissect the molecular signature of NFATc1-enriched articular cartilage progenitors. In order to minimize the influence of differentiated cells in GFP^+ and GFP^- cell

populations, single-clone cells were sorted at the first passage (P1), amplified for one more passage, and subjected to transcriptome analysis at P2 [Fig. 4(A)]. Bioinformatics analysis identified 117 high- and 168 low-expressing genes in GFP^+ *vs.* GFP^- cells [Fig. S3(A)]. High-expressing genes in GFP^+ cells were mainly related to skeletal system development, cartilage development, or extracellular matrix component and organization [Fig. 4(B) and Fig. S3(B)]. Of note, these high-expressing genes in GFP^+ cells included several previously reported articular cartilage progenitor cell markers[3, 23], such as *Osr2*, *Prg4*, *Postn*, *Col3a1*, *Gdf6*, and *Tgfbr2* [Fig. 4(C)]. In contrast, enriched genes in GFP^- cells were mainly relevant to muscle cell development and differentiation [Fig. S3(C)], suggesting that GFP^- single-clone cells could be skeletal muscle progenitors. Importantly, the characteristic molecular signature and enriched biological pathways in GFP^+ cells were verified by the second transcriptome analysis using bulk primary GFP^+ cells [Fig. S3(D-F)].

Cell surface markers are important in identifying and sorting progenitor or stem cells. Transcriptome analyses showed that both GFP^+ and GFP^- progenitors expressed several surface markers of cells of mesenchymal origin, including *Cd9*, *Sca1*, *Thy1*, *Cd73*, *Cd166*, and *Cd200*, but not hematopoietic or endothelial markers *Cd11b*, *Cd45*, or *Cd31* (Table S1). When compared with GFP^- cells, GFP^+ cells displayed higher expression of *Cd105*, *Cd10*, *Cd13* and lower expression of *Cd146*, *Cd29*, *Cd151* [Fig. 4(D)]. The expression of CD105, CD9, SCA1, CD166, CD200, CD11B, CD45, and CD31 were further verified by flow cytometry in GFP^+ and GFP^- cells [Fig. 4(E, F) and Fig. S4]. Combined, these data identify a set of genes preferentially expressed in NFATc1-expressing articular cartilage progenitors and provide a perspective to understand the transcriptional signature of these progenitors.

NFATc1 negatively regulates articular chondrocyte differentiation

The function of NFATc1 in articular cartilage progenitors remains unclear. As aforementioned, the lineage tracing of *Nfatc1*-expressing cells showed that most articular chondrocytes were GFP$^+$ in *Nfatc1-Cre;Rosa26-mTmG*$^{fl/+}$ mice at 8 weeks of age, but the real-time expression of NFATc1 was confined to the superficial layers of articular cartilage as shown by RFP expression after tamoxifen pulse in *Nfatc1-CreER*^{T2}*;Rosa26-RFP*$^{fl/+}$ mice [Fig. S1(C)]. These results indicate that NFATc1 expression was diminished with articular chondrocyte differentiation. Consistently, the diminishment of *Nfatc1* expression was also detected in *ex vivo* chondrogenesis in *Nfatc1*-expressing articular cartilage progenitors [Fig. 5(A)].

Next, we wondered whether suppressing NFATc1 expression in articular cartilage progenitors is sufficient to induce chondrocyte differentiation. To address this, we deleted NFATc1 expression in GFP$^+$ articular cartilage progenitors by CRISPR/CAS9 technique [Fig. S5]. Strikingly, the deletion of NFATc1 expression was enough to induce chondrocyte differentiation without adding the chondrogenic medium as shown by alcian blue staining and induced expression of *Acan*, *Col2a1,* and *Col10a1* [Fig. 5(B)]. In the meantime, overexpression of NFATc1 in GFP$^+$ progenitor cells inhibited chondrocyte differentiation [Fig. 5(C) and Fig. S5].

To verify the function of NFATc1 in regulating articular chondrogenesis *in vivo*, we conditionally deleted *Nfatc1* in *Prrx1*-expressing limb mesenchymal progenitors by crossing *Prrx1-Cre* mice with *Nfatc1*$^{fl/fl}$ mice. The staining for articular cartilage was markedly strengthened in *Prrx1-Cre;Nfatc1*$^{fl/fl}$ (homozygous) *vs. Prrx1-Cre;Nfatc1*$^{fl/+}$ (heterozygous) mice [Fig. 5(D, E)]. Consistently, the expression of *Acan*, *Col2a1*, and *Col10a1* genes was significantly upregulated in the articular cartilage of *Prrx1-Cre;Nfatc1*$^{fl/fl}$ mice [Fig. 5(F)]. Notably, the articular cartilage consisted of mostly round, large chondrocytes in *Prrx1-Cre;Nfatc1*$^{fl/fl}$ mice, instead of the normal transitional alignment from the superficial layer to deep layers [Fig. 5(E)].

The volume changes of articular chondrocytes resulted in an increased thickness of articular cartilage in *Prrx1-Cre;Nfatc1*$^{fl/fl}$ *vs. Prrx1-Cre;Nfatc1*$^{fl/+}$ mice [Fig. 5(E)]. These results indicate that the *in vivo* deletion of *Nfatc1* in limb mesenchymal progenitors promotes articular chondrocyte differentiation as well.

Based on gene expression changes after deleting or overexpressing NFATc1, *Col2a1* turned out to be one of the most significantly changed chondrocyte-related genes we examined [Fig. 5(B, C, F) and reference[22]]. To understand the mechanism of NFATc1 regulating articular chondrocyte differentiation, we performed computational screening and identified a total of 38 potential NFAT binding sites across the upstream 6k base pairs of exon 1 and the intron 1 of mouse *Col2a1* gene [Fig. 5(G)], suggesting that NFATc1 might play a role in regulating *Col2a1* gene transcription. Indeed, luciferase analysis showed that silence or overexpression of NFATc1 markedly upregulated or downregulated the transcriptional activity of *Col2a1,* respectively [Fig. 5(H)]. Therefore, NFATc1 negatively determines articular chondrocyte differentiation at least partly through regulating the transcription of the COL2A1 gene.

Discussion

For quite a long period, the interzone cells have been considered as the origin of articular chondrocytes[2, 24]. Also, progenitor cells in the flanking mesenchyme surrounding the joint interzone were found to migrate into the interzone region and form articular cartilage[5, 6, 25, 26]. The current obscurity in identifying the precise origin of articular chondrocytes could be attributed to the lack of a specific molecular marker to distinguish cells in the flanking region from interzone cells. From this perspective, the limited expression of NFATc1 in the flanking region at the primary stage of mouse knee development [E13.5, Fig. 1(A, E) and Fig. S1(A)] provides a unique opportunity to track progenitors in the flanking region during articular cartilage development. The progressive pattern of NFATc1-expressing cells contributing to articular cartilage formation (Figs. 1-2) suggests that NFATc1-expressing progenitors in the flanking region may represent the origin of articular chondrocytes. Further studies into the spatiotemporal roadmap of NFATc1-expressing progenitor cell development are essential to elucidate the landscape of articular cartilage formation. Notably, these results also demonstrate that NFATc1 can constantly track articular cartilage progenitors throughout embryonic development and postnatal growth.

Transcriptome analyses in both single-clone and bulk primary cells reveal that NFATc1-expressing articular cartilage cells enrich several previously identified articular cartilage progenitor cell markers including *Osr2*, *Prg4*, *Postn*, *Col3a1*, and *Gdf6* [Fig. 4(C)][3, 23], therefore advocating their identity as articular cartilage progenitors. In addition, cell surface molecules including CD105, CD13, CD10, CD9, SCA1, CD166 can be considered as complementary markers for identifying and screening articular cartilage progenitors. Most impressively, NFATc1-expressing articular cartilage progenitors enrich a set of genes like *Fbn2*, *Piezo2*,

Dchs1, *Enpp1*, *Gdf6*, *Fgf9*, *Trps1*, *Col27a1*, *Tgfbr2*, *Col1a1*, and *Col1A2* [Fig. 4(B)], whose mutations have been linked to a diverse range of human musculoskeletal disorders (https://www.omim.org). These findings suggest that the dysfunction of articular cartilage progenitors may underlie these human musculoskeletal disorders. Of note, we did not detect the expression of *Gdf5* in articular cartilage progenitors from neonatal mice, which coincides with previous reports that *Gdf5* is greatly diminished with synovial joint development and undetectable in the articular cartilage of neonatal mice[3, 27, 28]. However, the enriched expression of *Gdf6* may provide a complementary role to *Gdf5* [Fig. 4(B)][29]. Together, these results provide important insights into the molecular signature of articular cartilage progenitors.

Our results show that suppression of NFATc1 is sufficient to induce articular chondrogenesis both *ex vivo* and *in vivo* [Fig. 5(B, D-F)] and thus NFATc1 could represent a core negative transcriptional regulator of articular chondrocyte differentiation. Notably, this role of NFATc1 in regulating chondrocyte differentiation is confined to the articular cartilage because NFATc1 does not express in growth-plate progenitors or chondrocytes [Fig. 1(A, E) and Fig. S1(A)]. Consistent with the inhibitory role of NFATc1 in articular chondrocyte differentiation, previous *in vitro* studies in murine chondrogenic cell line ATDC5 cells and human epiphyseal chondrocytes also showed that NFATc1 suppresses chondrocyte differentiation[30].

Notably, a protective role of NFATc1 in osteoarthritic cartilage has been suggested previously, which is based on the decrease of NFATc1 expression in lesional osteoarthritic cartilage in human patients, as well as the severe articular cartilage deterioration in mice with conditional deletion of *Nfatc1* driven by the Collagen 2 promoter Cre with a background of *Nfatc2* deficiency (*Nfatc1*^{Col2}*;Nfatc2*$^{-/-}$ mice)[21, 31]. While the *Nfatc1*^{Col2}*;Nfatc2*$^{-/-}$ mice indeed develop osteoarthritic phenotypes, we did not find the typic osteoarthritic phenotype in the follow-up study in mice

with deletion of *Nfatc1* driven by tamoxifen-induced *Aggrecan-CreER*^{T2} with the background of *Nfatc2* deficiency (*Nfatc1*^{AggrecanCreER}*;Nfatc2*$^{-/-}$ mice) after administering tamoxifen at different ages. Instead, these animals develop obvious osteochondroma-like lesions at the entheseal site and within ligaments around the joint[22]. Since *Col2* is also expressed in perichondrial precursors[14, 32], the accelerated osteoarthritis phenotype in *Nfatc1*^{Col2}*;Nfatc2*$^{-/-}$ mice could be secondary to the osteochondroma phenotype in these animals, instead of a direct beneficial role of NFATc1 in articular cartilage.

A recent study by Atsuta et al. using limb bud mesenchymal cells showed that the ectopic expression of NFATc1 seems to promote chondrocyte differentiation as shown by the alcian blue staining in micromass-cultured cells[33]. While additional experiments are necessary to confirm chondrocyte differentiation at the molecular level, overexpression of NFATc1 in cells from the whole limb bud might not reflect the physiological function of NFATc1 in chondrogenesis because NFATc1 expression is highly confined to articular and perichondrial progenitors during skeletal development according to the lineage tracing data in *Nfatc1-Cre* and *Nfatc1-CreER*^{T2} reporter mice (Figs.1,2 and reference[22]). Therefore, this disparity could also be due to the different cell types utilized in these two studies.

The mechanism of regulating NFATc1 expression during articular cartilage development remains unclear. A previous study showed that Notch signaling suppresses NFATc1 expression in ATDC5 cells and primary chondrocytes[30]. Furthermore, the Notch signaling can be activated by mechanical loading in mandibular condylar chondrocytes and bone marrow stromal cells[34, 35]. Therefore, it is possible that mechanical loading and Notch signaling act upstream of NFATc1 expression during articular cartilage development. Further studies need to verify this speculation and explore other biochemical, biophysical, and epigenetic pathways regulating

NFATc1 expression during articular chondrocyte differentiation. In addition, our transcriptome data show that *Nfatc4* is also enriched in articular cartilage progenitors. The function of NFATc4 and its relationship with NFATc1 in regulating articular cartilage formation needs further investigation.

In summary, we have unveiled that NFATc1-expressing progenitors generate articular but not growth-plate chondrocytes during development and identified NFATc1 as a critical negative transcriptional regulator of articular chondrocyte differentiation. Given the importance of NFATc1 in articular chondrogenesis, modulating NFAT signaling in skeletal progenitors may represent a novel, precise strategy for articular cartilage regeneration and treating cartilaginous diseases.

Limitations of the study

There are some important limitations to our present study. Firstly, the GFP^+ cells we used in this study might contain some cells not expressing NFATc1 but derived from NFATc1-expressing precursors. Given the prominent progenitor cell properties of the GFP^+ cell population, if these derived cells also display characteristics of progenitor cells, their precursors (NFATc1-expressing cells) will represent a higher hierarchy of progenitors or stem cells, which yet support our conclusions. In fact, NFATc1 is positively expressed in the incipient articular cartilage of neonatal mice [Fig. 1(E)] and these NFATc1-expressing cells can form local cell clusters with articular cartilage development [Fig. 2(A)], indicating that NFATc1 also marks articular cartilage progenitors in neonatal mice. Secondly, these GFP^+ cells might include cells from other articular tissues (e.g. meniscus, articular synovium). Since all articular tissues are derived from progenitor cells sharing the same molecular markers[1, 5] and currently there are no

specific markers to distinguish progenitors for these different articular tissues, it was challenging to explicitly isolate articular cartilage progenitor cells at the early stages of development. Future studies will be necessary to dissect the developmental hierarchy of NFATc1-expressing articular cartilage progenitor cells and elucidate the mechanisms determining their differentiation to meniscal or synovial cells versus articular chondrocytes. Thirdly, the detailed molecular mechanism of NFATc1 regulating articular chondrocyte differentiation needs further exploration. Future studies using techniques like ChIP-sequencing, CUT&RUN, or CUT&Tag will be able to unveil the transcriptional landscape of NFATc1-regulated articular chondrocyte differentiation.

Methods

Mouse lines

The *Nfatc1*$^{tm1.1(cre)Bz}$ (*Nfatc1*^{Cre})[36] strain and *Nfatc1*$^{tm1.1(cre/ERT2)Bzsh}$ (*Nfatc1-CreER*^{T2})[37] strain were a generous gift from Dr. Bin Zhou (Albert Einstein College of Medicine) and Dr. Bin Zhou (Shanghai Institutes for Biological Sciences, Chinese Academy of Sciences), respectively. The B6(Cg)-*Nfatc1*^{tm3Glm}/AoaJ (*Nfatc1*^{fl})[18], B6.Cg-Tg(Prrx1-cre)1Cjt/J (*Prrx1*^{Cre})[38], *Gt(ROSA)26 Sor*$^{tm4(ACTB-tdTomato,-EGFP)Luo}$ (*Rosa26-mTmG*^{fl})[39], and *Gt(ROSA)26Sor*$^{tm9(CAG-tdTomato)Hze}$ (*Rosa26-RFP*^{fl})[40] mice were obtained from The Jackson Laboratory. Severe combined immune deficient (SCID) beige mice were acquired from Beijing Vital River Laboratory Animal Technology Co., Ltd. All mice were housed under the standard barrier facility on a 12-h light/dark cycle with ad libitum access to water and regular chow. All experiments were approved by Institutional Animal Care and Use Committee.

Tamoxifen (T5648, Sigma-Aldrich) was administered by intraperitoneal injection at 1 mg/10 g body weight for adult mice and 0.5 mg/10 g body weight for 2-week-old or dam mice. To induce Cre recombination in *Nfatc1-CreER*^{T2}*;Rosa26-RFP*$^{fl/+}$ mice at 2 weeks and 8 weeks of age, tamoxifen was injected for 5 consecutive days, which was confirmed to induce a high recombination efficiency of *CreER*^{T2} in mouse articular cartilage[22].

Histology and confocal microscopy imaging

Limb samples at different ages (n = 3-5 mice for each age, two knee joints per animal) were fixed in 4% paraformaldehyde and processed for serial frozen sections at 8-10 μm thickness. The expression of GFP or RFP was observed using a Leica SP8 confocal microscope.

For quantifying GFP or RFP positive cells in articular cartilage, the KEYENCE BZ-X710 fluorescence microscope and software were used under the 40x objective and cell count module. Slides were selected every 100 μm, and five slides were used for each sample (*n* = 5 *Nfatc1-Cre;Rosa26-mTmG*$^{fl/+}$ mice, 3 *Nfatc1-CreER*^{T2}*;Rosa26-RFP*$^{fl/+}$ mice). The total number of cells in each tissue was counted by combining the DAPI stain with cell morphology under phase contrast. The number of GFP+ or RFP+ cells was counted by combining the green or red fluorescence with DAPI. The percentage of GFP+ or RFP+ cells for each articular tissue was calculated by dividing the number of GFP+ or RFP+ cells by the total number of cells. The average of five slices from each sample was considered as the percentage of GFP$^+$ or RFP$^+$ cells in the sample.

Cell culture and sorting

Cells were isolated from the knee of neonatal *Nfatc1-Cre;Rosa26-mTmG*$^{fl/+}$ mice. Briefly, after removing the skin and most surrounding muscle tissue, the mouse knee was minced into small fragments and digested with 3 mg/ml collagenase type I (Worthington) and 4 mg/ml dispase (Roche) in complete culture media for 15 min at 37 °C. After digestion, cells were passed through a 70 μm strainer and cultured for seven days. GFP$^+$ and GFP$^-$ cells were sorted using a FACSAria™ Fusion or FACSAria™ II cell sorter (BD Bioscience).

Ex vivo assays of cell colony formation

For cell colony formation assay, single-cell suspensions of GFP$^+$ and GFP$^-$ cells (*n* = 6 with cells from 3 mice, two replicates for each) were plated in 6-well-plates at indicated densities and cultured for two weeks. Cells were fixed in 10% neutral formalin for 15 min and stained in 1% crystal violet for 5 min. Clone numbers (> 50 cells) were counted and scored blindly under the microscope.

Ex vivo assays of osteogenic and adipogenic differentiation

The same number of cells were plated in 6-well-plates and cultured for two weeks in complete growth media for colony formation. Differentiation media were added to induce osteogenesis (αMEM supplemented with 10% FBS, 10 nM dexamethasone, 50 μg/ml L-ascorbic acid, and 10 mM β-glycerophosphate) for 4 weeks or adipogenesis (αMEM supplemented with 10% FBS, 100 nM dexamethasone, 50 μM indomethacin, 5 ug/ml insulin) for 10 days. Calcium nodules and fat were visualized by staining with alizarin red and Oil Red O respectively. Total cell clones with positive staining were blindly counted under the microscope. The expression of osteogenic or adipogenic marker genes was examined by quantitative PCR.

Ex vivo assay of chondrogenic differentiation

The cell pellet 3-dimension (3D) culture system for ex vivo chondrogenesis was as previously described[41]. Briefly, cells (1 x 10^6) were pelleted in 15 ml polypropylene tubes by centrifugation and cultured in chondrogenic media [DMEM high glucose supplemented with 2% FBS, 100 nM dexamethasone, 50 μg/ml L- ascorbic acid, 1% insulin, transferrin, selenium (ITS), 1 mM sodium pyruvate, 40 μg/ml L-proline, and 10 ng/ml TGF-β1] for 3 weeks. The pellets were fixed in 10% formalin and processed for paraffin embedding. Chondrogenesis was displayed by alcian blue staining and COL2A1 immunohistochemistry.

For micromass culture, 2 x10^6 cells in 20 ul media were dropped in the center of a well in the 24-well-plate. After incubating for 2 hours, complete culture media was added and cultured overnight. Chondrogenic media was added the next day to start the induction of chondrogenesis. Chondrogenic differentiation was evaluated by alcian blue staining and the expression of chondrocyte-associated genes.

In vivo cell transplantation

GFP^+ or GFP^- cells (2.0×10^6) mixed with Matrigel (200 µl, BD Biosciences) were injected into the dorsal skin of SCID beige mice (*n* = 6 animals per group). Transplants were harvested after 4 weeks and fixed in 10% formalin for histological analyses. The formation of calcified cartilage in GFP^+ cells was determined by two experienced pathologists based on the hematoxylin stain and the hardness of the tissue when making sections.

Immunohistochemistry

Paraffin-embedded sections (*n* = 3 mice, two knee joints per animal for NFATc1 expression analysis or 6 cell pellets for COL2A1 expression analysis, 3-5 serial slides per sample) were digested with pepsin for 15 min at 37 °C. Primary anti-Collagen Type II monoclonal antibody (clone 6B3, Millipore), anti-NFATc1 (clone 7A6, Santa Cruz), or the isotype control mouse IgG1 (Biolegend) was incubated using a M.O.M. kit (Vector Laboratories). Sections were counterstained using Hematoxylin.

Quantitative PCR

Total RNA was isolated using the QIAzol lysis reagent. RNA samples were treated with an RNase-Free DNase Set (QIAGEN), and equal amounts (1 µg) were used for reverse transcriptase reaction using random primers (AffinityScript QPCR cDNA Synthesis Kit). PCR primer sequences are listed in Table S2. All gene expression was normalized to housekeeping genes *Gapdh* and presented by$2^{-\Delta Ct}$ or $2^{-\Delta\Delta Ct}$ [42].

RNA preparation for transcriptome analysis

Total RNA was isolated from single-cell clone or bulk GFP^+ and GFP^- cells (n = 3 with cells from three different mice in each group) using QIAzol lysis reagent (Qiagen). DNA was removed using the RNase-Free DNase Set (QIAGEN). RNA was quantified with Nanodrop 2000. The integrity of RNA was evaluated using an Agilent Bioanalyzer 2100 (Agilent Technologies) and agarose gel electrophoresis.

Library preparation and RNA-sequencing (RNA-seq)

One microgram of total RNA from each sample was subjected to cDNA library construction using a NEBNext® Ultra non-directional RNA Library Prep Kit for Illumina® (New England Biolabs). Briefly, mRNA was enriched using oligo(dT) beads followed by two rounds of purification and fragmented randomly by adding the fragmentation buffer. The first-strand cDNA was synthesized using random hexamers primer, after which a custom second-strand synthesis buffer (Illumina), dNTPs, RNase H, and DNA polymerase I were added to generate the second-strand (ds cDNA). After a series of terminal repairs, polyadenylation, and sequencing adaptor ligation, the double-stranded cDNA library was completed following size selection and PCR enrichment.

The resulting 250-350 bp insert libraries were quantified using a Qubit 2.0 fluorometer (Thermo Fisher Scientific) and quantitative PCR. The size distribution was analyzed using the Agilent Bioanalyzer 2100. The equal amount of each RNA-Seq library was sequenced on an Illumina HiSeq 4000 Platform (Illumina) using a paired-end 150 run (2 x 150 bases).

Bioinformatics analysis

Paired-end clean reads were aligned to mouse genome GRCm38/mm10 using STAR (v2.5)[43]. HTSeq v0.6.1 was used to count the read numbers mapped of each gene. And then

FPKM of each gene was calculated based on the length of the gene and read counts mapped to this gene[44]. Differential expression analysis between two groups was performed using the DESeq2 R package (2_1.6.3)[45]. The resulting P-values were adjusted using Benjamini and Hochberg's approach for controlling the False Discovery Rate (FDR). Genes with an adjusted P-value < 0.05 found by DESeq2 were assigned as differentially expressed. Gene Ontology (GO) enrichment analysis of differentially expressed genes was implemented by the clusterProfiler R package[46], in which gene length bias was corrected. GO terms with an adjusted P value less than 0.05 were considered to be significant.

Flow cytometry

The following antibodies of cell surface molecules were used: Allophycocyanin (APC) anti-mouse CD45 (clone 30-F11, eBioscience), anti-mouse CD31 (clone 390, Biolegend), anti-mouse CD166 (EbioALC48, eBioscience), anti-mouse CD200 (clone OX-90, Biolegend), anti-mouse SCA1 (clone E13-161.7, Biolegend), anti-mouse CD105 (clone MJ7/18, Biolegend), APC Rat IgG2a, κ isotype control antibody (clone RTK2758, Biolegend), APC Rat IgG2b, κ isotype control antibody (clone RTK4530, Biolegend), APC Rat IgG1, κ isotype control (clone RTK2071, Biolegend); Alexa Fluor 647 anti-mouse CD9 (clone MZ3, Biolegend), Alexa Fluor 647 Rat IgG2a, κ isotype control antibody (clone RTK2758, Biolegend).

Cells (n = 3 with cells from three different mice) were stained with antibodies or IgG isotype controls for 30 min at room temperature. Stained cells were analyzed on a FACSCalibur™ or BD LSR II flow cytozmeter (BD Bioscience). Positive cells were gated based on both unstained and isotype-matched IgG stained cells. Data analysis was performed using FlowJo software (Tree Star Inc.).

CRISPR/Cas9 lentivirus production

Pairs of CRISPR guide RNA oligos (*Nfatc1* single guide RNA [sgRNA] targeting TACGAGCTTCGGATCGAGGT on exon 3) were annealed and cloned into the BsmBI sites of lentiCRISPR V2-blasticidin vector (a gift from Dr. Lizhi He at Harvard Medical School). CRISPR lentiviral plasmid and lentiviral packaging plasmids (pMDLg/pRRE, pRSV-Rev, and pMD2.G; Addgene) were transfected into 293T cells. Supernatants were harvested and filtered through a 0.45-μm filter 2.5 days after transfection. GFP^+ cells were infected with *Nfatc1*-CRISPR lentivirus. The lentivirus infected cells were selected using 5 μg/ml blasticidin for five days before further analyses.

caNFATc1 Retrovirus production

The retroviral expression vectors pMSCV-GFP and pMSCV-caNFATc1 have been previously described[47]. Recombinant retroviruses were produced by co-transfecting either the pMSCV-GFP or pMSCV-caNFATc1 vectors together with retroviral packing plasmids gag/pol and pVSV-G (Addgene) into Phoenix cells using Effectene Transfection Reagent (QIAGEN). Supernatants were harvested and filtered through a 0.45-μm filter 48 hours after transfection. GFP^+ cells were infected by adding retroviral supernatant with 4 μg/ml polybrene for 72 hours before further analyses.

Western Blotting

Western blotting was performed using 4–20% Mini-PROTEAN® TGX™ precast protein gels with the following antibodies anti-NFATc1 (1:1000, clone 7A6, Santa Cruz) and anti-GAPDH (1:2000, Cell Signaling Technology). Fifty micrograms of protein were loaded for each sample.

Luciferase assay

The transcription activity of *Col2a1* was determined by co-transfecting ATDC5 cells, which had been infected with *Nfatc1*-CRISPR lentivirus or caNFATc1 retrovirus, with 1 g of the reporter plasmid (pGL2B-COL2-6.5E309, a gift from Dr. Mary Goldring) and 10 ng of pRL Renilla luciferase plasmid using the Effectene transfection reagent (Qiagen). Cells were transfected for 8 hrs and then cultured for 24 hrs. The activity of the Firefly luciferase was measured and normalized to Renilla luciferase activity using the Dual-Luciferase Reporter Assay System (Promega).

Statistical analyses

All data are presented as mean ± *s.d.*. The normality and the equal variance of data sets were tested using the Shapiro-Wilk test and F test, respectively. Data were determined to be normally distributed and have equal variance unless specified otherwise. Differences between the two groups were evaluated by the two-tailed Student's *t*-test. For counting data of cell colonies, comparisons were performed using the nonparametric Mann-Whitney test. Analyses of multiple groups were performed using two-way ANOVA followed by Sidak's test for between-group comparisons. All analyses were performed using Prism 9.2.1 (GraphPad).

Acknowledgments

We thank Dr. Antonios Aliprantis for helpful discussions and critically reading the manuscript; Dr. Ruirui Shi for collecting parts of these data; Dr. Lizhi He for generating the CRISPR/CAS9 lentivirus; Dr. Yidong Wang for assistance in obtaining the *Nfatc1-Cre* mouse strain, Dr. Yulong He for assistance in obtaining the *Nfatc1-CreER*^{T2} mouse strain, and Drs. Guangchuang Yu and Haibo Liu for suggestions of statistical analysis.

Contributions

XG conceived the project, designed all experiments, interpreted the results, and wrote the manuscript. FZ, MW, and XG performed experiments. YZ provided critical support for the project. BZ (New York) and BZ (Shanghai) provided the *Nfatc1-Cre* and *Nfatc1-CreER* mouse strains, respectively.

Funding source

This study was supported by National Natural Science Foundation of China (project 81100767 to Dr. Ge), Beijing Natural Science Foundation (project 5222008 to Dr. Ge), Natural Science Foundation of Capital Medical University (project 1220010146 to Dr. Ge), Ministry of Education of China (project 2092808 to Dr. Ge), and two Young Researcher Awards (Dr. Ge).

Competing interest

The authors declare no conflict of interest.

References

1. Koyama E, Shibukawa Y, Nagayama M, Sugito H, Young B, Yuasa T, et al. A distinct cohort of progenitor cells participates in synovial joint and articular cartilage formation during mouse limb skeletogenesis. Dev Biol 2008; 316: 62-73.
2. Chijimatsu R, Saito T. Mechanisms of synovial joint and articular cartilage development. Cell Mol Life Sci 2019; 76: 3939-3952.
3. Decker RS. Articular cartilage and joint development from embryogenesis to adulthood. Semin Cell Dev Biol 2017; 62: 50-56.
4. Rountree RB, Schoor M, Chen H, Marks ME, Harley V, Mishina Y, et al. BMP receptor signaling is required for postnatal maintenance of articular cartilage. PLoS Biol 2004; 2: e355.
5. Shwartz Y, Viukov S, Krief S, Zelzer E. Joint Development Involves a Continuous Influx of Gdf5-Positive Cells. Cell Rep 2016; 15: 2577-2587.
6. Decker RS, Um HB, Dyment NA, Cottingham N, Usami Y, Enomoto-Iwamoto M, et al. Cell origin, volume and arrangement are drivers of articular cartilage formation, morphogenesis and response to injury in mouse limbs. Dev Biol 2017; 426: 56-68.
7. Chagin AS, Medvedeva EV. Regenerative medicine: Cartilage stem cells identified, but can they heal? Nat Rev Rheumatol 2017; 13: 522-524.
8. Coles JM, Zhang L, Blum JJ, Warman ML, Jay GD, Guilak F, et al. Loss of cartilage structure, stiffness, and frictional properties in mice lacking PRG4. Arthritis Rheum 2010; 62: 1666-1674.
9. Rhee DK, Marcelino J, Baker M, Gong Y, Smits P, Lefebvre V, et al. The secreted glycoprotein lubricin protects cartilage surfaces and inhibits synovial cell overgrowth. J Clin Invest 2005; 115: 622-631.

10. Kozhemyakina E, Zhang M, Ionescu A, Ayturk UM, Ono N, Kobayashi A, et al. Identification of a Prg4-expressing articular cartilage progenitor cell population in mice. Arthritis Rheumatol 2015; 67: 1261-1273.

11. Li T, Longobardi L, Myers TJ, Temple JD, Chandler RL, Ozkan H, et al. Joint TGF-beta type II receptor-expressing cells: ontogeny and characterization as joint progenitors. Stem Cells Dev 2013; 22: 1342-1359.

12. Lefebvre V, Dvir-Ginzberg M. SOX9 and the many facets of its regulation in the chondrocyte lineage. Connect Tissue Res 2017; 58: 2-14.

13. Haseeb A, Kc R, Angelozzi M, de Charleroy C, Rux D, Tower RJ, et al. SOX9 keeps growth plates and articular cartilage healthy by inhibiting chondrocyte dedifferentiation/osteoblastic redifferentiation. Proc Natl Acad Sci U S A 2021; 118: e2019152118.

14. Akiyama H, Kim JE, Nakashima K, Balmes G, Iwai N, Deng JM, et al. Osteo-chondroprogenitor cells are derived from Sox9 expressing precursors. Proc Natl Acad Sci U S A 2005; 102: 14665-14670.

15. Hogan PG, Chen L, Nardone J, Rao A. Transcriptional regulation by calcium, calcineurin, and NFAT. Genes Dev 2003; 17: 2205-2232.

16. Vaeth M, Feske S. NFAT control of immune function: New Frontiers for an Abiding Trooper. F1000Res 2018; 7: 260.

17. Mancini M, Toker A. NFAT proteins: emerging roles in cancer progression. Nat Rev Cancer 2009; 9: 810-820.

18. Aliprantis AO, Ueki Y, Sulyanto R, Park A, Sigrist KS, Sharma SM, et al. NFATc1 in mice represses osteoprotegerin during osteoclastogenesis and dissociates systemic osteopenia from inflammation in cherubism. J Clin Invest 2008; 118: 3775-3789.

19. Takayanagi H. The role of NFAT in osteoclast formation. Ann N Y Acad Sci 2007; 1116: 227-237.

20. Koga T, Matsui Y, Asagiri M, Kodama T, de Crombrugghe B, Nakashima K, et al. NFAT and Osterix cooperatively regulate bone formation. Nat Med 2005; 11: 880-885.

21. Greenblatt MB, Ritter SY, Wright J, Tsang K, Hu D, Glimcher LH, et al. NFATc1 and NFATc2 repress spontaneous osteoarthritis. Proc Natl Acad Sci U S A 2013; 110: 19914-19919.

22. Ge X, Tsang K, He L, Garcia RA, Ermann J, Mizoguchi F, et al. NFAT restricts osteochondroma formation from entheseal progenitors. JCI Insight 2016; 1: e86254.

23. Bian Q, Cheng YH, Wilson JP, Su EY, Kim DW, Wang H, et al. A single cell transcriptional atlas of early synovial joint development. Development 2020; 147: dev185777.

24. Rux D, Decker RS, Koyama E, Pacifici M. Joints in the appendicular skeleton: Developmental mechanisms and evolutionary influences. Curr Top Dev Biol 2019; 133: 119-151.

25. Niedermaier M, Schwabe GC, Fees S, Helmrich A, Brieske N, Seemann P, et al. An inversion involving the mouse Shh locus results in brachydactyly through dysregulation of Shh expression. J Clin Invest 2005; 115: 900-909.

26. Koyama E, Ochiai T, Rountree RB, Kingsley DM, Enomoto-Iwamoto M, Iwamoto M, et al. Synovial joint formation during mouse limb skeletogenesis: roles of Indian hedgehog signaling. Ann N Y Acad Sci 2007; 1116: 100-112.

27. Francis-West PH, Abdelfattah A, Chen P, Allen C, Parish J, Ladher R, et al. Mechanisms of GDF-5 action during skeletal development. Development 1999; 126: 1305-1315.

28. Merino R, Macias D, Ganan Y, Economides AN, Wang X, Wu Q, et al. Expression and function of Gdf-5 during digit skeletogenesis in the embryonic chick leg bud. Dev Biol 1999; 206: 33-45.

29. Settle SH, Jr., Rountree RB, Sinha A, Thacker A, Higgins K, Kingsley DM. Multiple joint and skeletal patterning defects caused by single and double mutations in the mouse Gdf6 and Gdf5 genes. Dev Biol 2003; 254: 116-130.

30. Zanotti S, Canalis E. Notch suppresses nuclear factor of activated T cells (NFAT) transactivation and Nfatc1 expression in chondrocytes. Endocrinology 2013; 154: 762-772.

31. Beier F. NFATs are good for your cartilage! Osteoarthritis Cartilage 2014; 22: 893-895.

32. Ono N, Ono W, Nagasawa T, Kronenberg HM. A subset of chondrogenic cells provides early mesenchymal progenitors in growing bones. Nat Cell Biol 2014; 16: 1157-1167.

33. Atsuta Y, Tomizawa RR, Levin M, Tabin CJ. L-type voltage-gated Ca(2+) channel CaV1.2 regulates chondrogenesis during limb development. Proc Natl Acad Sci U S A 2019; 116: 21592-21601.

34. Ziouti F, Ebert R, Rummler M, Krug M, Muller-Deubert S, Ludemann M, et al. NOTCH Signaling Is Activated through Mechanical Strain in Human Bone Marrow-Derived Mesenchymal Stromal Cells. Stem Cells Int 2019; 2019: 5150634.

35. Yan F, Feng J, Yang L, Shi C. The effect induced by alternated mechanical loading on Notch-1 in mandibular condylar cartilage of growing rabbits. Bone Joint Res 2021; 10: 437-444.

36. Wu B, Zhang Z, Lui W, Chen X, Wang Y, Chamberlain AA, et al. Endocardial cells form the coronary arteries by angiogenesis through myocardial-endocardial VEGF signaling. Cell 2012; 151: 1083-1096.

37. Tian X, Hu T, Zhang H, He L, Huang X, Liu Q, et al. Vessel formation. De novo formation of a distinct coronary vascular population in neonatal heart. Science 2014; 345: 90-94.

38. Logan M, Martin JF, Nagy A, Lobe C, Olson EN, Tabin CJ. Expression of Cre Recombinase in the developing mouse limb bud driven by a Prxl enhancer. Genesis 2002; 33: 77-80.

39. Muzumdar MD, Tasic B, Miyamichi K, Li L, Luo L. A global double-fluorescent Cre reporter mouse. Genesis 2007; 45: 593-605.

40. Madisen L, Zwingman TA, Sunkin SM, Oh SW, Zariwala HA, Gu H, et al. A robust and high-throughput Cre reporting and characterization system for the whole mouse brain. Nat Neurosci 2010; 13: 133-140.

41. Embree MC, Chen M, Pylawka S, Kong D, Iwaoka GM, Kalajzic I, et al. Exploiting endogenous fibrocartilage stem cells to regenerate cartilage and repair joint injury. Nat Commun 2016; 7: 13073.

42. Schmittgen TD, Livak KJ. Analyzing real-time PCR data by the comparative C(T) method. Nat Protoc 2008; 3: 1101-1108.

43. Dobin A, Davis CA, Schlesinger F, Drenkow J, Zaleski C, Jha S, et al. STAR: ultrafast universal RNA-seq aligner. Bioinformatics 2013; 29: 15-21.

44. Trapnell C, Williams BA, Pertea G, Mortazavi A, Kwan G, van Baren MJ, et al. Transcript assembly and quantification by RNA-Seq reveals unannotated transcripts and isoform switching during cell differentiation. Nat Biotechnol 2010; 28: 511-515.

45. Anders S, Huber W. Differential expression analysis for sequence count data. Genome Biol 2010; 11: R106.

46. Yu G, Wang LG, Han Y, He QY. clusterProfiler: an R package for comparing biological themes among gene clusters. OMICS 2012; 16: 284-287.

47. Horsley V, Aliprantis AO, Polak L, Glimcher LH, Fuchs E. NFATc1 balances quiescence and proliferation of skin stem cells. Cell 2008; 132: 299-310.

Figure legends

Fig. 1 Articular cartilage is derived from NFATc1-expressing progenitors.

(A) Confocal microscopy images showing the distribution of GFP$^+$ cells during articular cartilage development at the knee of *Nfatc1-Cre;Rosa26-mTmG*$^{fl/+}$ mice (*n* = 5 animals for each age, 2 knee joints per animal). Arrow indicating the main location of GFP$^+$ cells at the knee at embryonic day 13.5 (E13.5). P0, postnatal day 0. (B) Quantification of GFP$^+$ cells in the articular cartilage of *Nfatc1-Cre;Rosa26-mTmG*$^{fl/+}$ mouse knee at 8 weeks of age (*n* = 5 animals, one knee joint per animal). AC, articular cartilage. (C) Representative confocal images demonstrating the distribution of RFP$^+$ cells in the articular cartilage at 2 weeks and 8 weeks of age in *Nfatc1-CreER*^{T2}*;Rosa26-RFP*$^{fl/+}$ mice 48 hrs after tamoxifen pulse for 5 consecutive days (*n* = 3 mice for each age, 2 knee joints per animal). (D) Quantification of RFP$^+$ cells in the articular cartilage of *Nfatc1-CreER*^{T2}*;Rosa26-RFP*$^{fl/+}$ mouse knee at 2 weeks and 8 weeks of age (*n* = 3 mice for each age, one knee joint per animal). (E) Immunohistochemistry detecting the expression of NFATc1 during mouse articular cartilage development (*n* = 3 mice for each age, 2 knee joints per animal). Data are mean ± *s.d.* of results from 5 or 3 animals; scale bars, 200 μm except for the right 3 images in (E), 50 μm.

Fig. 2 NFATc1-expressing progenitors form cell clusters with articular cartilage development and contribute to the meniscus and articular synovium formation.

(A) Confocal microscopy images showing the distribution of GFP$^+$ cells in the articular cartilage of *Nfatc1-CreER*^{T2}*;Rosa26-mTmG*$^{fl/+}$ mouse knee at 1 week and 8 weeks after administering tamoxifen to dams at P0 and P1. The most left image showing GFP$^+$ cells in articular tissues after 1 week of tamoxifen administration. The right 3 images demonstrating GFP$^+$ cell clusters in the articular cartilage (arrows) and meniscus (arrowheads). (B) Representative confocal

images displaying GFP$^+$ cells or cell clusters (arrows) in the meniscus and articular synovium at 1 week or 2 weeks after tamoxifen administration to dams at P0 and P1. (C) Confocal microscopy images demonstrating that GFP$^+$ cells contribute to the formation of the synovial lining (left image, arrowheads, 2 weeks of age) and the patella of the knee (right image, arrow, P0) in *Nfatc1-Cre;Rosa26-mTmG*$^{fl/+}$ mice. All images are representative of 5 mice at each time point or age, 2 knee joints per animal. Scale bars, 200 μm.

Fig. 3 Colony formation and multipotent differentiation of *Nfatc1*-expressing progenitors. (A) Schematic diagram showing culturing and sorting GFP$^+$ and GFP$^-$ cells from the knee of neonatal *Nfatc1-Cre;Rosa26-mTmG*$^{fl/+}$ mice. (B) Colony formation assay of GFP$^+$ and GFP$^-$ cells with 50 or 100 cells plated in 6-well-plates and cultured for two weeks. *n* = 6 with cells from 3 animals, two replicates for each, nonparametric Mann-Whitney test; experiment repeated twice. (C) Alcian blue staining and immunohistochemistry of COL2A1 showing the chondrogenic potential of GFP$^+$ and GFP$^-$ cell pellets after being cultured in the chondrogenic differentiation medium for 3 weeks. Isotype as a negative control for COL2A1 antibody. The maximum diameter of cell pellets reflecting the proliferative capacity of GFP$^+$ and GFP$^-$ cells. *n* = 9 with cells from 3 animals, three replicates for each. (D) Alizarin red staining and gene expression analysis of *Ibsp* and *Sp7* demonstrating the osteogenic potential of GFP$^+$ and GFP$^-$ cells after being cultured in the osteogenic differentiation medium for 4 weeks. *n* = 6 with cells from 3 animals, two replicates for each, nonparametric Mann-Whitney test for colony counting data, two-way ANOVA followed by Sidak's tests for gene expression data; experiments repeated twice. (E) Oil red staining and gene expression analysis of *Fabp4* and *Lpl* displaying adipogenesis in GFP$^+$ and GFP$^-$ cells after being cultured in the adipogenic differentiation medium for 10 days. *n* = 6 with cells from 3 animals, two replicates for each, nonparametric Mann-Whitney test for colony counting data, two-way ANOVA followed by Sidak's tests for gene

expression data; experiments repeated twice. (F) Schematic illustration and histology respectively showing transplantation of GFP^+ cells along with Matrigel matrix underneath the dorsal skin of severe combined immune-deficient mice and the formation of chondrocytes, chondrocyte clusters, and calcified cartilage (arrows) 4 weeks later. Images are representative of 6 animals, with GFP^- cells as the control (results shown in Fig. S2B). All data are mean ± *s.d.*. Scale bars, 400 μm (C), 500 μm (D), 200 μm (E, F).

Fig. 4 Transcriptional profile of *Nfatc1*-expressing articular cartilage progenitors.

(A) Schematic diagram showing the process of sorting single-clone cells for RNA-sequencing. (B) Cluster heatmap displaying 20 high-expressing genes associated with articular cartilage development in GFP^+ *vs.* GFP^- cells. Color descending from red to blue indicates log10(FPKM+1) from large to small. *n* = 3 with cells from 3 animals in each group. (C) Transcriptome analysis revealing the enrichment of previously reported articular cartilage progenitor marker genes *Osr2*, *Prg4*, *Postn*, *Col3a1*, and *Tgfbr2* in GFP^+ relative to GFP^- cells. (D) Transcriptome analysis identifying high expression of *Cd105*, *Cd10*, *Cd13* and low expression of *Cd146*, *Cd29*, *Cd151* in GFP^+ *vs.* GFP^- cells. (E) Flow cytometry verifying the expression of CD105 in GFP^+ relative to GFP^- cells. (F) Flow cytometry showing the expression of cell surface molecules CD9, SCA1, CD166, and CD200 in GFP^+ and GFP^- cells. Representative results of cells from 3 mice, experiment repeated twice.

Fig. 5 NFATc1 negatively determines articular chondrocyte differentiation through regulating *Col2a1* gene transcription.

(A) Gene expression analysis displaying the change of *Nfatc1* expression in GFP^+ cell-micromass cultured in the chondrogenic medium for 10 days. *n* = 3, experiment repeated three times with cells from 3 mice. (B) Alcian blue staining and gene expression analysis of *Acan*,

Col2a1, and *Col10a1* after deleting *Nfatc1* by CRISPR/CAS9 technique in *ex vivo* micromass culture of GFP$^+$ cells from neonatal *Nfatc1-Cre;Rosa26-mTmG*$^{fl/+}$ mice (day 7, without chondrogenic induction, *n* = 3). Experiment repeated three times with cells from 3 animals. (C) Quantification of alcian blue staining and gene expression analysis of *Col2a1* and *Col10a1* showing decreased chondrogenesis after overexpressing NFATc1 in GFP$^+$ cells by infecting a caNFATc1 retrovirus structure. For alcian blue staining, *n* = 6 with cells from 3 animals, two replicates for each; for gene expression analysis, *n* = 3, experiment repeated twice with cells from 2 animals. (D) Safranin O staining demonstrating enhanced articular cartilage staining in the hip of *Prrx1-Cre;Nfatc1*$^{fl/fl}$ *vs. Prrx1-Cre;Nfatc1*$^{fl/+}$ mice at 12 weeks of age. Representative images from 5 animals in each group were displayed. (E) Representative images of alcian blue staining and polarized light on H&E staining manifesting increased staining (arrows) and thickness of articular cartilage (double arrows) in the knee of *Prrx1-Cre;Nfatc1*$^{fl/fl}$ relative to *Prrx1-Cre;Nfatc1*$^{fl/+}$ mice at 16 weeks of age. *n* = 5 animals for each group. (F) Quantitative PCR determining the expression of *Acan*, *Col2a1*, and *Col10a1* genes in articular cartilage of *Prrx1-Cre;Nfatc1*$^{fl/fl}$ relative to *Prrx1-Cre;Nfatc1*$^{fl/+}$ mice at 8 weeks of age. *n* = 6 animals for each group. (G) Computational screening of NFAT binding sites on mouse *Col2a1* promoter and intron 1 sequences by PROMO software recognizing 38 putative NFAT binding sites across -6k bp of the promoter and intron 1. The transcriptional starting site is counted as +1. Location is given in bp relative to the transcriptional starting site. (G) Luciferase assay of transcriptional activity of *Col2a1* after deleting or overexpressing NFATc1 in ATDC5 cells. *n* = 3, experiment repeated three times. All data shown as mean ± s.d., two-tailed Student's *t*-test performed. Scale bar, 200 μm (D), 100 μm (E).

Supplementary figure legends

Fig. S1 Track NFATc1-expressing progenitors during articular cartilage development.

(A) Representative confocal image showing the distribution of GFP$^+$ cells at the prospective joint site of *Nfatc1-CreER^{T2};Rosa26-mTmG$^{fl/+}$* mice at E13.5 (*n* = 5 mouse embryos). Tamoxifen was administrated to pregnant dams at E11.5 and mouse limbs were sampled at E13.5. Arrows indicating locations of GFP$^+$ cells. (B) Histological images displaying immunostaining of IgG isotype control at different ages of mouse knee development (*n* = 3 mice each age, 2 knee joints per animal, related to Fig. 1E) (C) Representative confocal images showing the distribution of GFP$^+$ or RFP$^+$ cells in articular cartilage of *Nfatc1-Cre;Rosa26-mTmG$^{fl/+}$* (*n* = 5, two knee joints for each) or *Nfatc1-CreER^{T2};Rosa26-RFP$^{fl/+}$* (*n* = 3, two knee joints for each) mice respectively at 8 weeks of age. (D) Confocal images showing the absence of GFP$^+$ cells in articular cartilage of *Rosa26-mTmG$^{fl/+}$* control mice and *Nfatc1-CreER^{T2};Rosa26-mTmG$^{fl/+}$* mice without tamoxifen induction (*n* = 3 animals for each). Scale bars, 200 μm except for the right 3 images in (B), 50 μm.

Fig. S2 Colony formation and multipotent differentiation of *Nfatc1*-expressing progenitors.

(A) Colony formation assay of GFP$^+$ and GFP$^-$ cells at P5 with 100 cells plated in 6-well-plates and cultured for two weeks (*n* = 6 with cells from 3 mice, two replicates for each, nonparametric Mann-Whitney test). (B) Representative histology images demonstrating H&E staining of transplants of GFP$^-$ cells with Matrigel matrix underneath the dorsal skin of severe combined immune-deficient mice for 4 weeks. *n* = 6 animals; scale bars, 200 μm.

Fig. S3 Transcriptional profile of *Nfatc1*-expressing articular cartilage progenitors.

(A) Volcano diagram from transcriptome analysis of single clone-derived cells showing the distribution of differential expression genes in GFP^+ *vs.* GFP^- cells. The threshold of differential expression genes is *padj* < 0.05. (B) Histogram demonstrating top 20 significantly enriched pathways of high-expressing genes in GFP^+ relative to GFP^- cells by GO enrichment analysis. Green and red hearts referring to pathways related to extracellular matrix biology and skeletal system development respectively. (C) Histogram demonstrating top 20 significantly enriched pathways of enriched genes in GFP^- *vs.* GFP^+ cells by GO enrichment analysis. Yellow arrows indicating pathways related to skeletal muscle development. (D) Volcano diagram from transcriptome analysis of bulk primary GFP^+ cells showing the distribution of differential expression genes in GFP^+ *vs.* GFP^- cells. *padj* < 0.05 as the threshold of differential expression genes. (E) Cluster heatmap of RNA-sequencing results from bulk primary GFP^+ cells verifying the 20 high-expressing genes associated with skeletal and cartilage development in GFP^+ *vs.* GFP^- cells. Color descending from red to blue indicates log10(FPKM+1) from large to small. (F) Histogram demonstrating top 20 significantly enriched pathways of high-expressing genes in bulk primary GFP^+ cells relative to GFP^- cells by GO enrichment analysis. Green and red hearts as indicated in (B). *n* = 3 with cells from three different animals in each group. The n-numbers in (B), (C), and (F) indicating the number of differentially expressed genes concerning the GO term.

Fig. S4 Flow cytometry determining the expression of cell surface markers.

(A) Expression of CD11B, CD45, CD31 in GFP^+ and GFP^- cells from neonatal *Nfatc1-Cre;Rosa26-mTmG*$^{fl/+}$ mouse knee, IgG isotype as the negative control. Representative results of cells from 3 animals, experiment repeated twice. (B) A representative gating strategy for flow cytometry.

Fig. S5 Western blotting determining the deletion or overexpression of NFATc1 by lentiviral CRISPR/CAS9 or retroviral caNFATc1, respectively. The empty vector without a gRNA sequence was used as the control for CRISPR/CAS9 lentivirus production and infection. The pMSCV-GFP vector (Retro-GFP) was utilized as the control for caNFATc1 retrovirus production and infection.

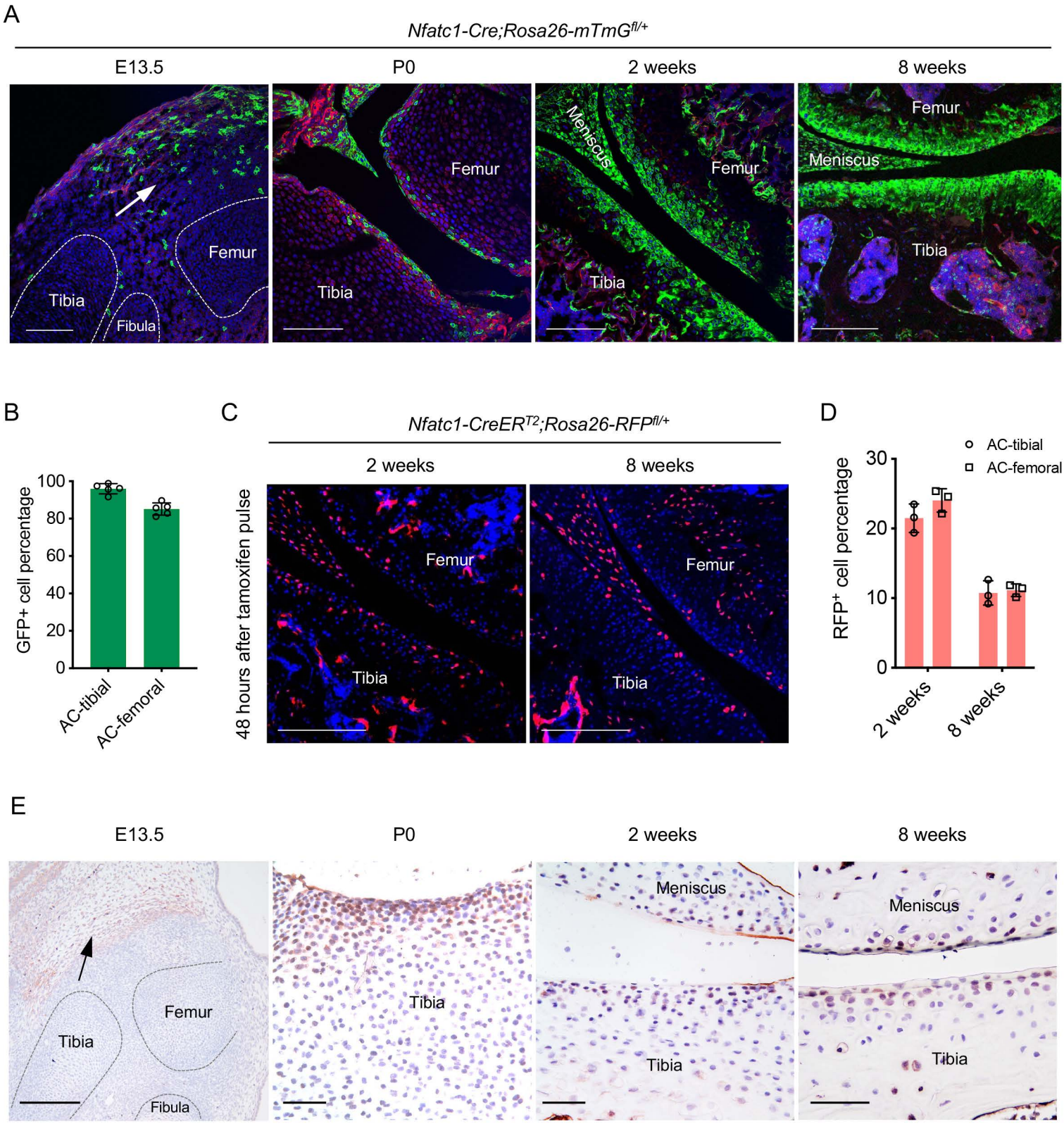

Figure 1

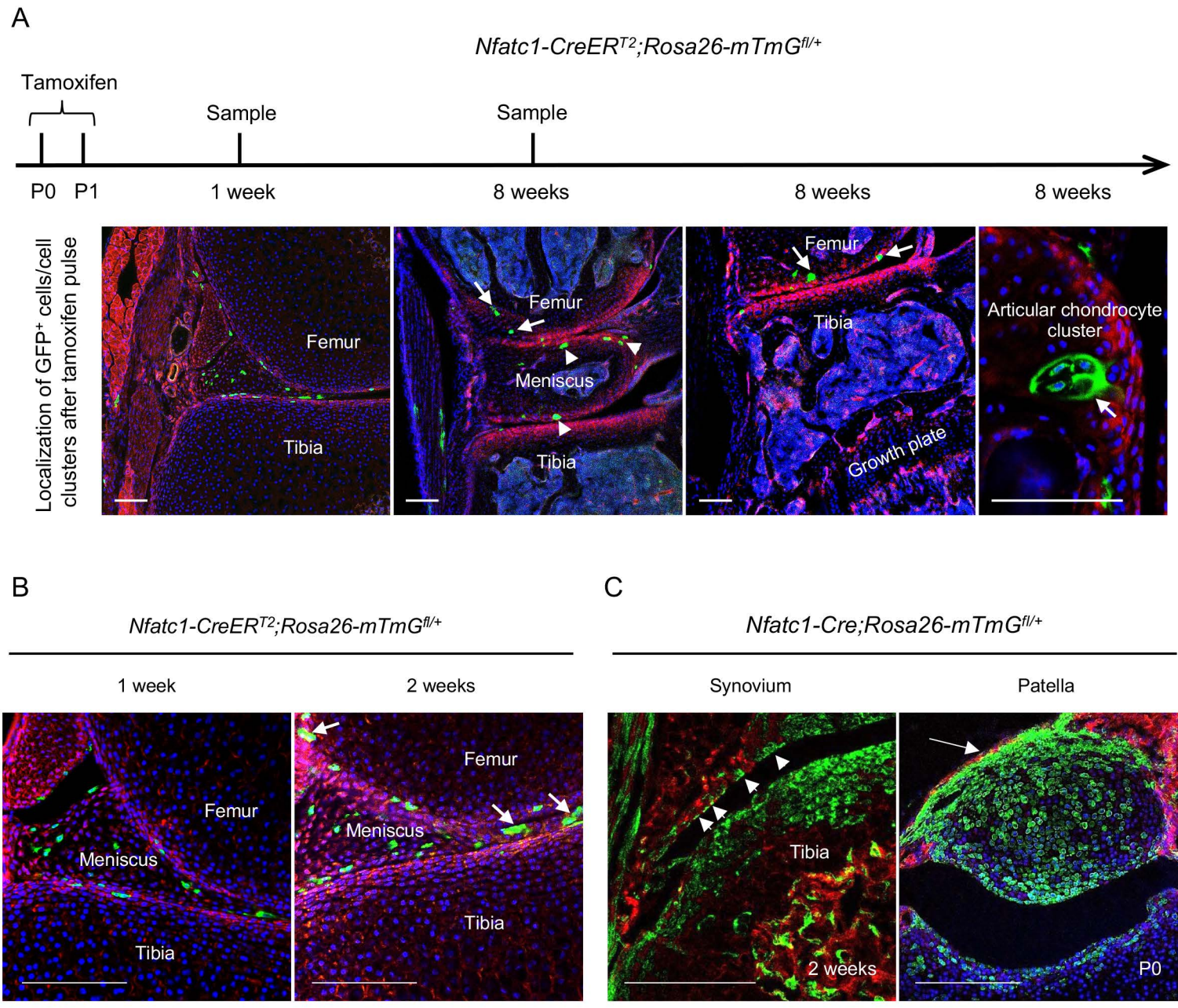

Figure 2

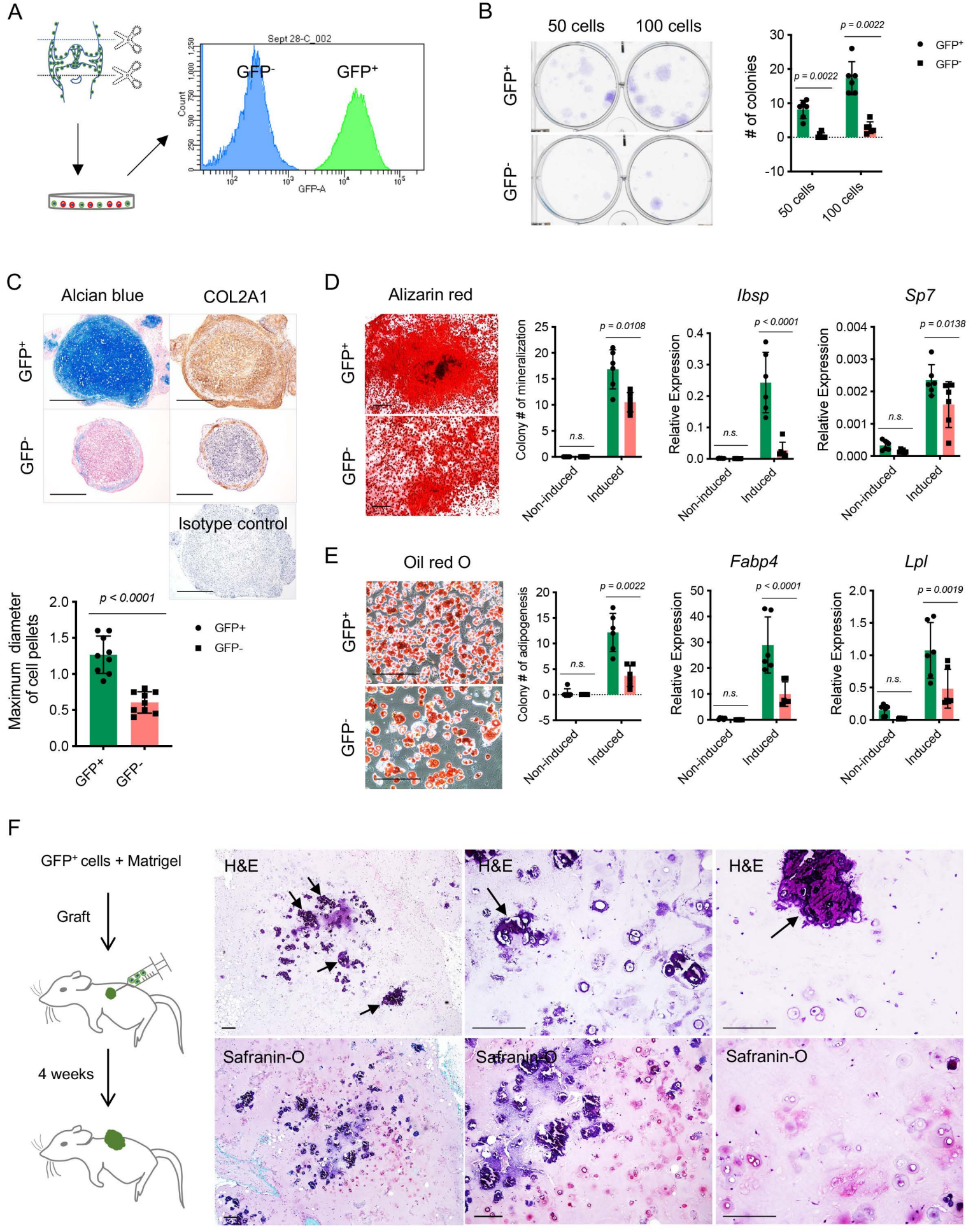

Figure 3

A

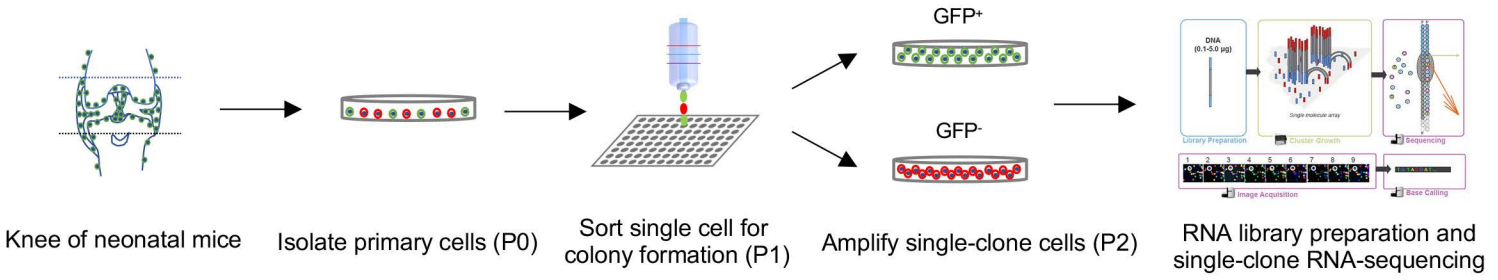

B

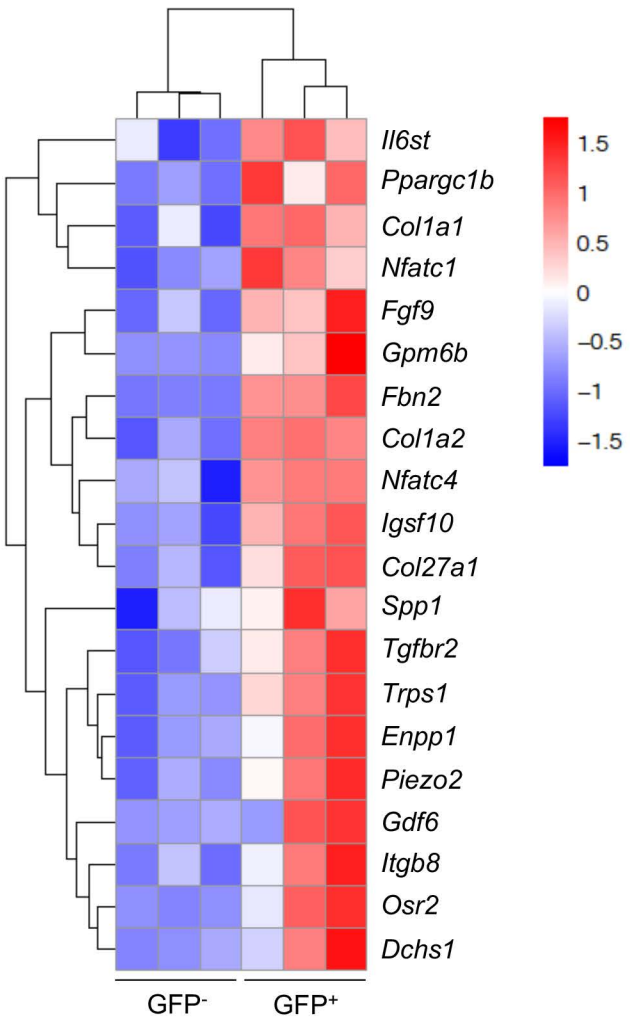

C

Enrichment of articular cartilage/joint stem cell markers in GFP$^+$ *vs.* GFP$^-$ cells

Gene Name	Fold Change	Adjusted *P* Value
Osr2	9.58	1.13E-09
Prg4	4.01	0.00092443
Postn	3.76	0.00077081
Col3a1	3.58	7.14E-08
Tgfbr2	2.32	0.0020401

D

Expression of surface molecules in GFP$^+$ *vs.* GFP$^-$ cells

Gene Name	Fold Change	Adjusted P Vaues
Eng (Cd105)	6.24	3.29E-14
Mme (Cd10)	5.75	9.99E-06
Anpep (Cd13)	7.59	1.47E-07
Mcam (Cd146)	0.26	6.80E-06
Itgb1 (Cd29)	0.52	2.66E-03
Cd151	0.58	2.36E-02

E

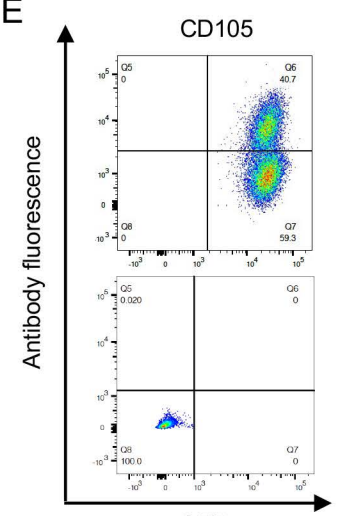

F

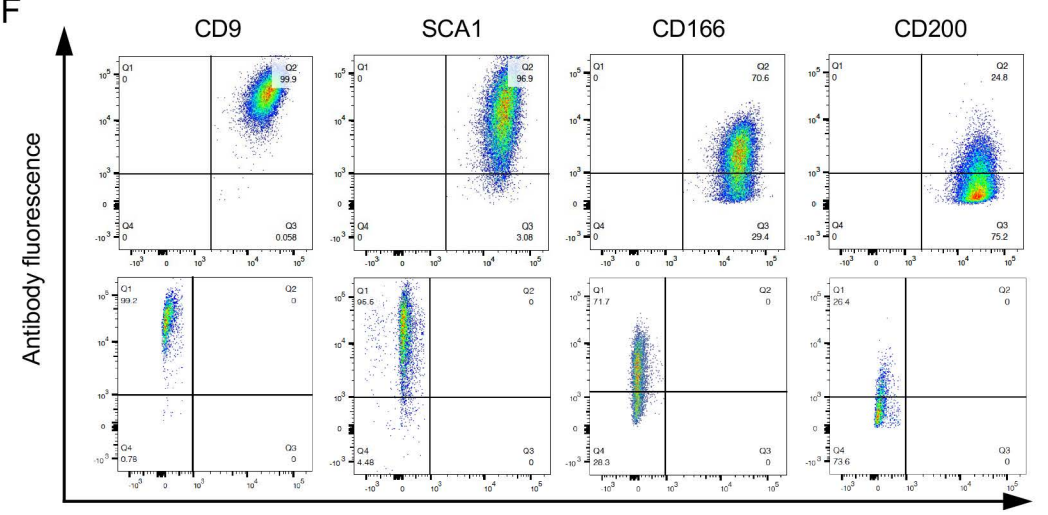

Figure 4

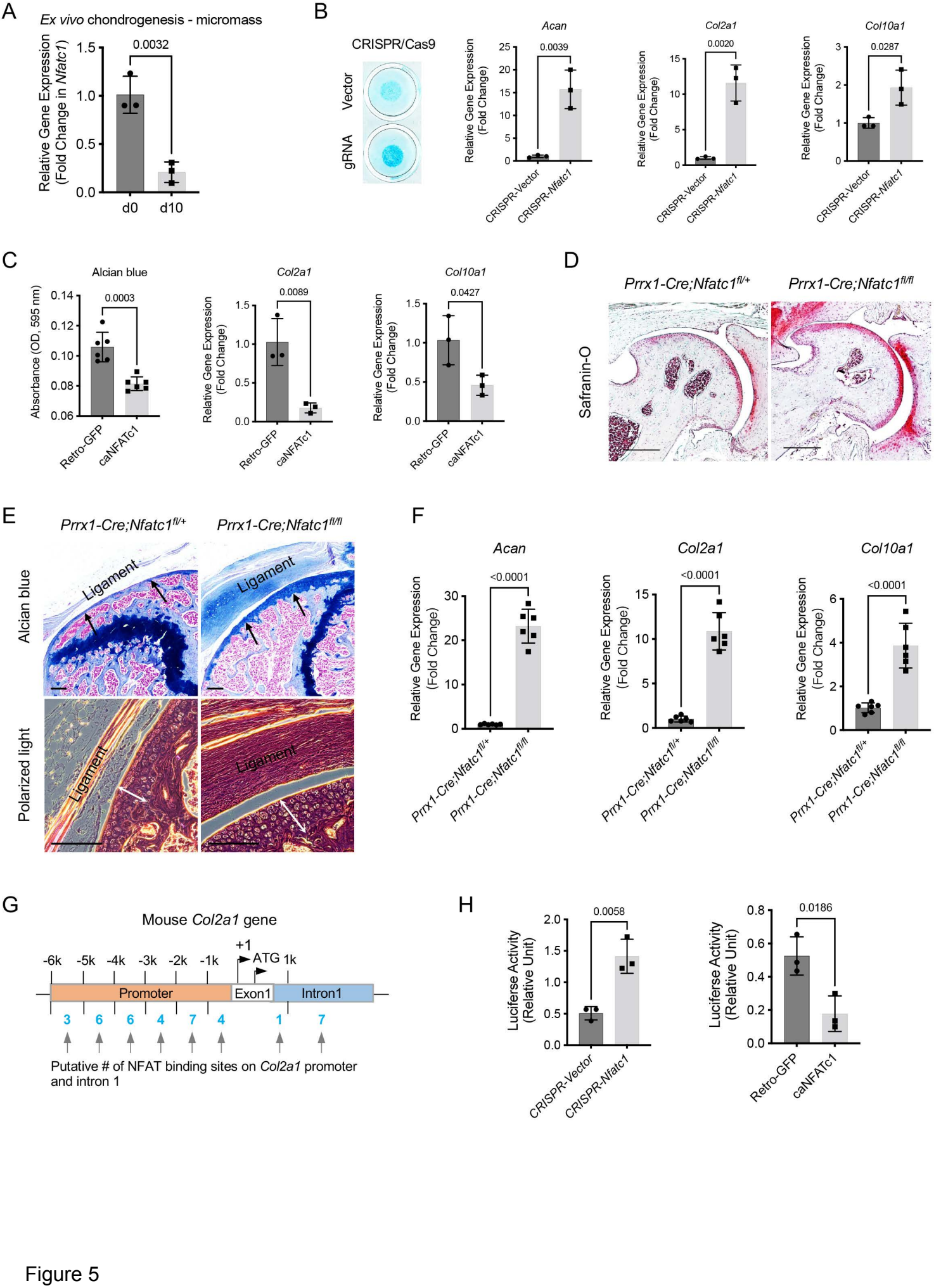

Figure 5

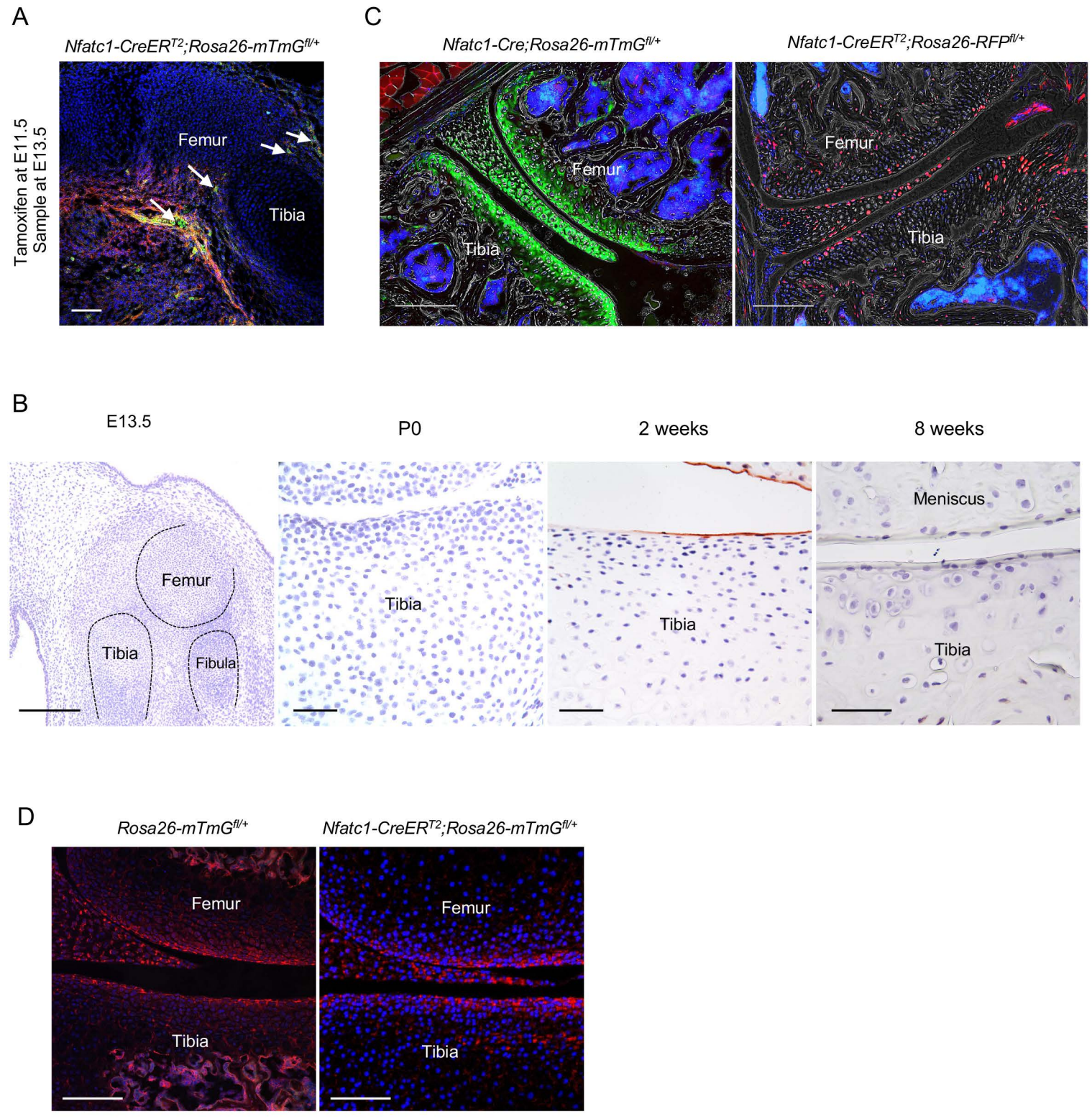

Figure S1

A

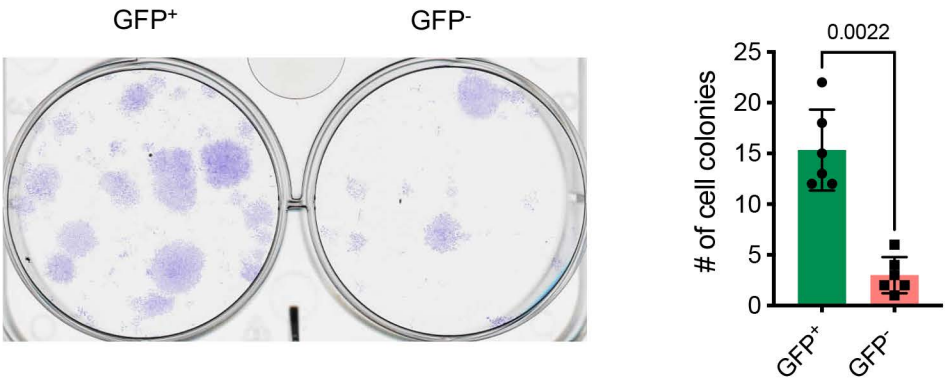

B

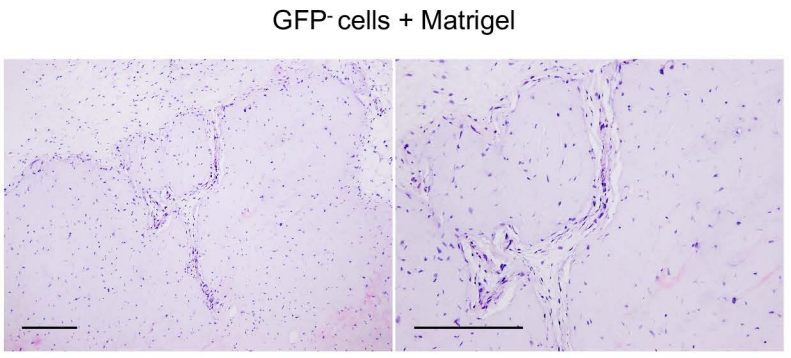

Figure S2

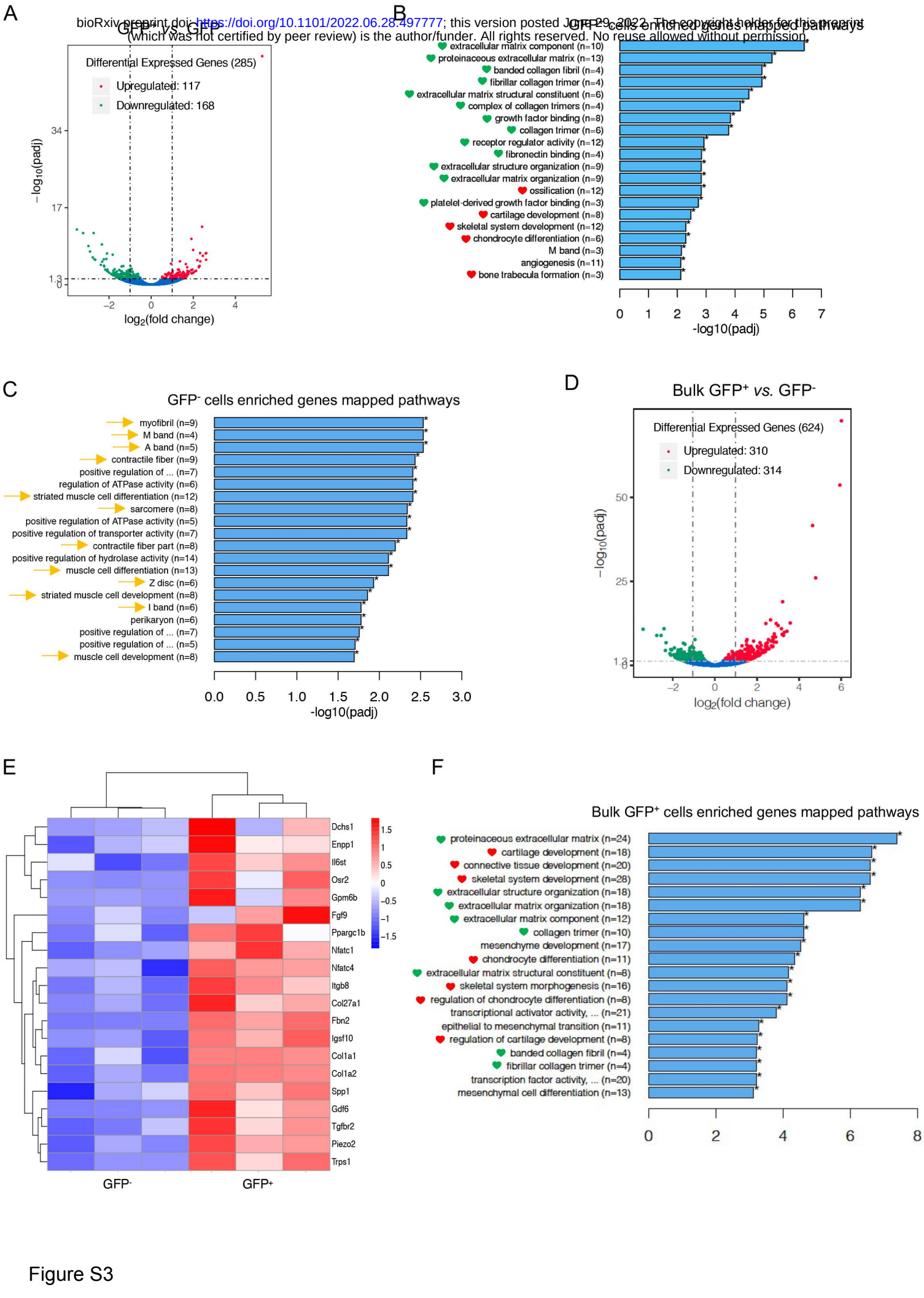

Figure S3

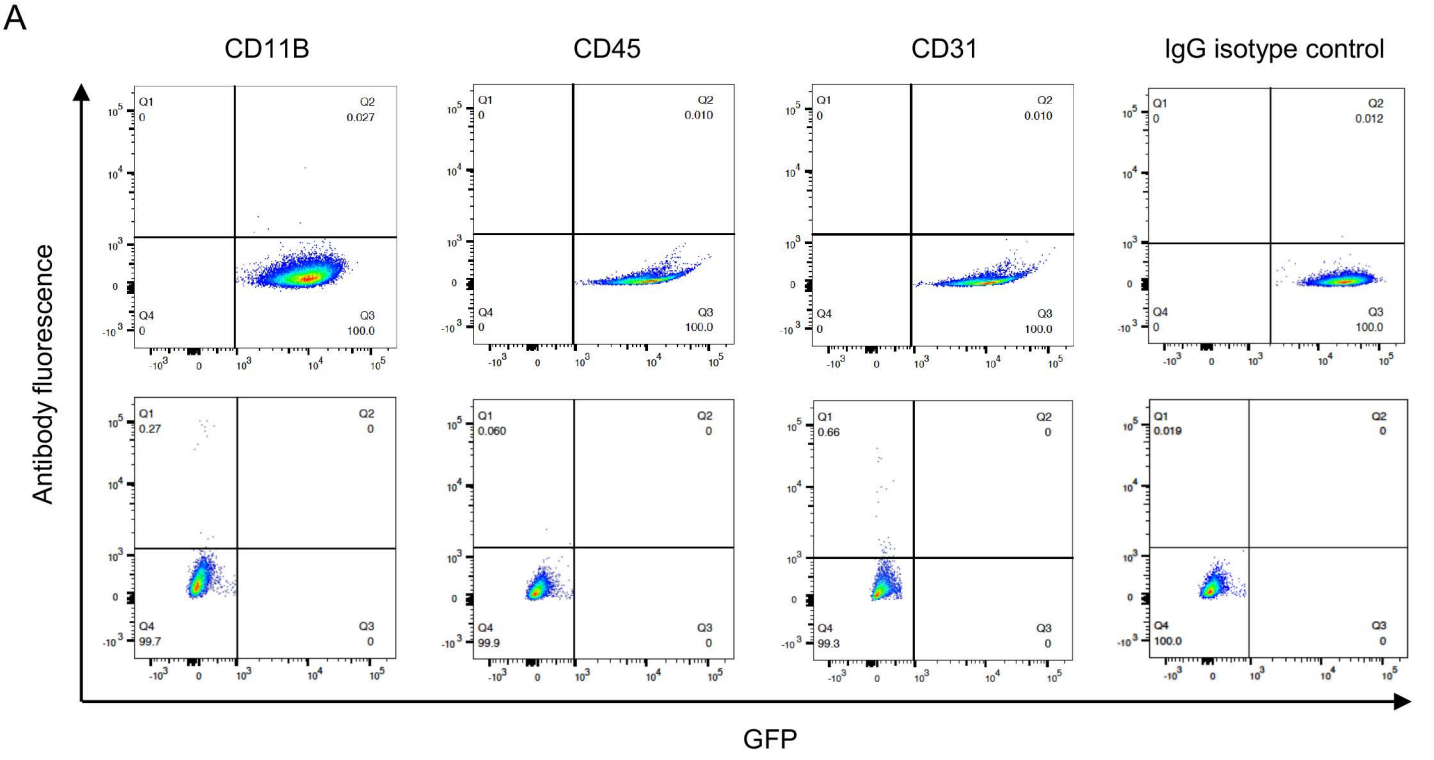

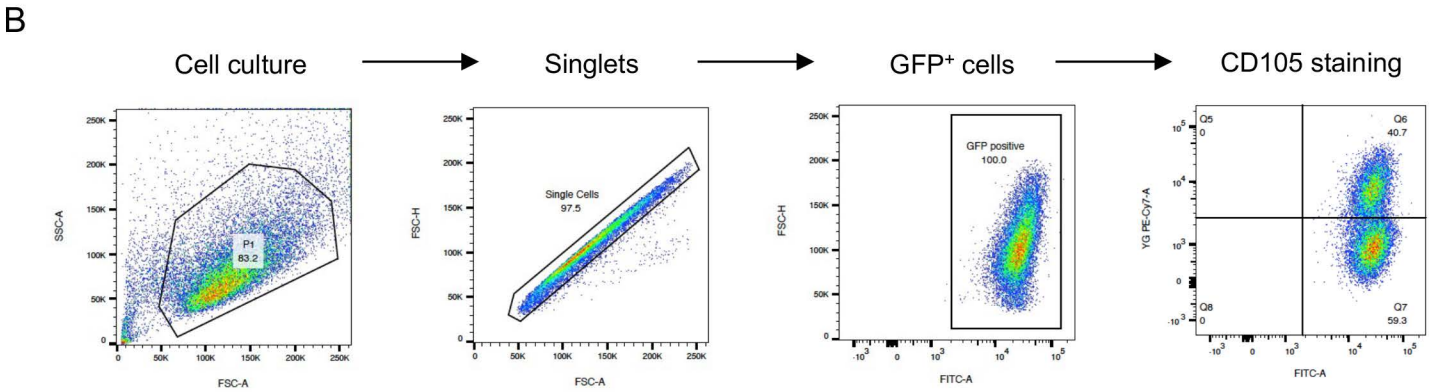

A representative gating strategy for antibody staining (CD105) of GFP+ cells

Figure S4

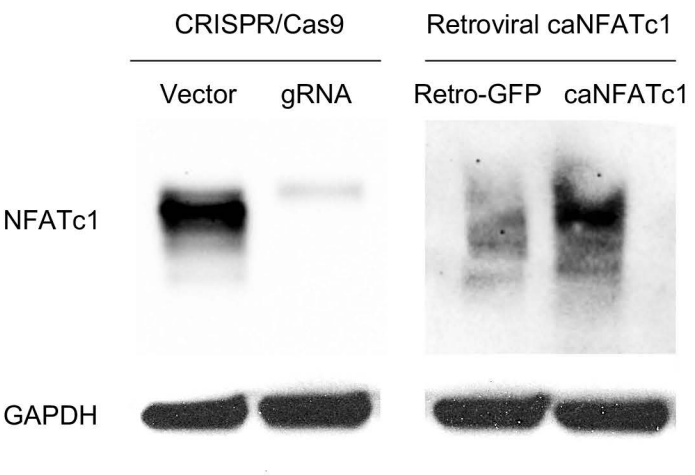

Figure S5

Table S1 Expression of cell surface markers in GFP^+ and GFP^- cells

ID	GeneName	GFP^+ 1_fpkm	GFP^+ 2_fpkm	GFP^+ 3_fpkm	GFP^- 1_fpkm	GFP^- 2_fpkm	GFP^- 3_fpkm
ENSMUSG00000030342	Cd9	65.24178361	170.3130261	52.25678967	22.27248396	57.26594193	142.3918025
ENSMUSG00000075602	Ly6a (Sca1)	70.79366524	105.3234945	98.89486333	37.1021049	693.6522093	205.219482
ENSMUSG00000032011	Thy1	140.7132316	303.3836654	254.7719782	151.4558484	651.9031186	319.4511689
ENSMUSG00000032420	Nt5e (Cd73)	1.72334916	0.981429803	5.238375478	2.377315109	0.325410005	0.461917023
ENSMUSG00000022636	Alcam (Cd166)	1.466182313	2.504226045	6.11752926	3.381415128	14.76002551	5.041349428
ENSMUSG00000022661	Cd200	1.602526526	1.65628498	3.25456675	1.735725289	1.194355761	3.209235421
ENSMUSG00000030786	Itgam (Cd11b)	0	0	0.007261888	0	0	0
ENSMUSG00000026395	Ptprc (Cd45)	0.032729627	0.00983166	0.030698709	0.006774711	0.029955456	0.027799249
ENSMUSG00000020717	Pecam1 (Cd31)	0	0.034771236	0.046304252	0	0.035418836	0.20794745

Data from transcriptome analyses (n = 3 mice per group). fpkm, fragments per kilobase of transcript sequence per million base pairs sequenced.

Table S2 Primer sequences for quantitative PCR

Gene	Forward primer	Reverse primer
Ibsp	AAAGTGAAGGAAAGCGACGA	GTTCCTTCTGCACCTGCTTC
Sp7	ATGGCGTCCTCTCTGCTTGA	GAAGGGTGGGTAGTCATTTG
Fabp4	AAGGTGAAGAGCATCATAACCCT	TCACGCCTTTCATAACACATTCC
Lpl	GGGAGTTTGGCTCCAGAGTTT	TGTGTCTTCAGGGGTCCTTAG
Nfatc1	CAACGCCCTGACCACCGATAG	GGCTGCCTTCCGTCTCATAGT
Acan	CTACAGAACAGCGCCATCAT	CTACAGAACAGCGCCATCAT
Col2a1	CGAGTGGAAGAGCGGAGAACT	AACTTTCATGGCGTCCAAGGT
Col10a1	TTCTGCTGCTAATGTTCTTGACC	GGGATGAAGTATTGTGTCTTGGG
Gapdh	TGCCAGCCTCGTCCCGTAGAC	CCTCACCCCATTTGATGTTAG